BOREAS An international journal of Quaternary research

Hässeldala – a key site for Last Termination climate events in northern Europe

Journal:	*Boreas*
Manuscript ID	BOR-030-2016.R2
Manuscript Type:	Original Article
Date Submitted by the Author:	17-Aug-2016
Complete List of Authors:	Wohlfarth, Barbara; Stockholm University, Geology and Geochemistry; Muschitiello, Francesco; Stockholm University, Geological Sciences Greenwood, Sarah; Stockholm University, Department of Geological Sciences Andersson, August; Stockholm University, Department of Applied Environmental Science Kylander, Malin; Stockholm University, Department of Geological Sciences Smittenberg, Rienk; Stockholm University, Geological Sciences Steinthorsdottir, Margret; Geological sciences Watson, Jenny; Queen's University Belfast, School of Geography, Archaeology and Palaeoecology Whitehouse, Nicola; Plymouth University, School of Geography, Earth and Environmental Sciences
Keywords:	Lateglacial climate, paleoenvironment, southern Sweden, lake sediments, Younger Dryas, multi-proxy studies

SCHOLARONE™ Manuscripts

Hässeldala – a key site for Last Termination climate events in northern Europe

BARBARA WOHLFARTH, FRANCESCO MUSCHITIELLO, SARAH GREENWOOD, AUGUST ANDERSSON, MALIN KYLANDER, RIENK H. SMITTENBERG, MARGRET STEINTHORSDOTTIR, JENNY WATSON AND NICOLA J. WHITEHOUSE

Wohlfarth, B., Muschitiello, F., Greenwood, S., Andersson, A., Kylander, M., Smittenberg, R. H., Steinthorsdottir, M., Watson, J. & Whitehouse, N. J.: Hässeldala – a key site for Last Termination climate events in northern Europe. *Boreas*...

For Review Only

The Last Termination (19 000-11 000 a BP) with its rapid and distinct climate shifts provides a perfect laboratory to study the nature and regional impact of climate variability. The sedimentary succession from the ancient lake at Hässeldala Port in southern Sweden with its distinct Lateglacial/early Holocene stratigraphy (>14.1-9.5 cal. ka BP) is one of the few chronologically well-constrained, multi-proxy sites in Europe that capture a variety of local and regional climatic and environmental signals. Here we present Hässeldala's multi-proxy records (lithology, geochemistry, pollen, diatoms, chironomids, biomarkers, hydrogen isotopes) in a refined age model and place the observed changes in lake status, catchment vegetation, summer temperatures and hydroclimate in a wider regional context. Reconstructed mean July temperatures increased between ~14.1 and ~13.1 cal. ka BP and subsequently declined. This latter cooling coincided with drier hydroclimatic conditions that were likely associated with a freshening of the Nordic Seas and started a few hundred years before the onset of Greenland Stadial 1 (~12.9 cal. ka BP). Our proxies suggest a further shift towards colder and drier conditions as late as ~12.7 cal. ka BP, which was followed by the establishment of a stadial climate regime (~12.5-11.8 cal. ka BP). The onset of warmer and wetter conditions led the Holocene warming over Greenland by ~200 years. Hässeldala's proxies thus highlight the complexity of environmental and hydrological responses across abrupt climate transitions in northern Europe.

Barbara Wohlfarth (barbara.wohlfarth@geo.su.se), Francesco Muschitiello, Sarah Greenwood, Malin Kylander, Rienk H. Smittenberg and Margret Steinthorsdottir, Department of Geological Sciences and Bolin Centre for Climate Research, Stockholm University, SE-10691, Stockholm, Sweden; August Andersson, Department of Applied Environmental Science and Bolin Centre for Climate Research, Stockholm University, SE-10691, Stockholm, Sweden; Jenny Watson, School of Geography, Archaeology and Palaeoecology, Queen's University Belfast, Belfast BT7 1NN, UK; Nicola J. Whitehouse, School of Geography, Earth and Environmental Sciences, Plymouth University, Drake Circus, Plymouth PL4 8AA, United Kingdom; *received 18th May 2016, accepted 18th August 2016.*

For Review Only

The transition period from the Last Glacial Maximum into the present Interglacial (the Holocene) occurred between 19 and 11 thousand years (ka) before present (BP) and is informally known as the 'Last Deglaciation' or the 'Last Termination'. This interval is characterised by a series of abrupt climate shifts of colder (stadial) and warmer (interstadial) states, which are most prominently expressed in the North Atlantic region (Björck *et al.* 1996; Lowe *et al.* 2008; Steffensen *et al.* 2008). These stadials and interstadials are often referred to as 'Oldest Dryas' (>14.7 ka BP), 'Bølling' (14.7-14.1 ka BP), 'Older Dryas' (14.1-13.9 ka BP), 'Allerød' (14.1-12.9 ka BP) and 'Younger Dryas' (12.9-11.7 ka BP) (Rasmussen *et al.* 2014) in reference to earlier pollen-stratigraphic work in Scandinavia (see e.g. Mangerud *et al.* 1974; Wohlfarth 1996).

Greenland ice core records have played a pivotal role in understanding the underlying causes of abrupt deglacial climate variability, because they (i) record climate shifts in a multitude of atmospheric proxies (Steffensen *et al.* 2008); (ii) provide a precise chronological template for past climatic events (Rasmussen *et al.* 2014); and (iii) can be synchronized to Antarctic ice cores using methane measurements (Blunier & Brook 2001). This synchronization allows for a direct correlation of Northern and Southern Hemisphere climatic changes and supports the hypothesis of the Atlantic bipolar seesaw concept (Broecker 1998), which attributes a large role to the Atlantic Meridional Overturning Circulation in triggering abrupt climate shifts (Stocker & Johnsen 2003; Knutti *et al.* 2004; EPICA 2006). The INTIMATE working group thus proposed to use the Greenland ice core isotope stratigraphy as a template against which marine and terrestrial records could be compared to decipher leads and lags between different regions (Björck *et al.* 1998; Walker *et al.* 1999). Unfortunately, rather than using independent chronological information to enable a critical appraisal of event sequences, many simply wiggle-matched their respective proxy stratigraphies to the Greenland ice core oxygen isotope curve. Lowe *et al.* (2008) and later Blockley *et al.* (2012) and Rasmussen *et al.* (2014) therefore refined the INTIMATE event stratigraphy by including cryptotephra layers that can be found in marine, ice core and terrestrial records and used as time-synchronous marker horizons. This latter approach has clear advantages as compared with simple wiggle-matching, but it soon became clear that a reliance only on cryptotephra layers to correlate between sites can be misleading as the ash may be reworked and/or originate from multiple eruptions of the same volcano with similar geochemical signatures (see e.g. Davies *et al.* 2004; Pyne-O'Donnell *et al.* 2008, 2010).

Although considerable advances have been made with respect to cryptotephra studies (Lowe *et al.* 2015) and radiocarbon calibration (Reimer *et al.* 2013), the lack of high-resolution, independent chronologies for terrestrial and marine records still makes it impossible to compare the exact regional and hemispheric phasing of Last Termination climatic events, albeit with a few exceptions (Lane *et al.* 2013; Lohne *et al.* 2013, 2014; Muschitiello & Wohlfarth 2015; Rach *et al.* 2014; Muschitiello *et al.* 2015b). Moreover, the detection of spatiotemporal differences of up to several hundred years in respect to temperature, precipitation, and vegetation changes both at the start of (Rach *et al.* 2014; Muschitiello & Wohlfarth 2015) and during Younger Dryas (Lane *et al.* 2013), suggests that the propagation of climatic signals on regional to sub-continental scales is still not fully understood. The assumption of more or less synchronous hydroclimatic and ecosystem responses even on regional scales is therefore clearly an oversimplification.

While chronological uncertainties surely play a major role when attempting to correlate between different archives (Blaauw 2012), the detection of past environmental and climatic shifts in various terrestrial archives also very much depends on (i) the choice of biological, chemical and physical proxies to be studied and their respective environmental and climatic information (e.g.,

For Review Only

seasonal temperature, precipitation, windiness, run-off, aquatic and terrestrial vegetation, lake status changes); (ii) understanding the complicated ecological processes that drive biotic and abiotic changes (e.g. Jackson & Overpeck 2000; Ammann *et al.* 2013; Birks & Birks 2014) and lake development (Engstrom *et al.* 2000); and (iii) the transfer functions and other methods used to derive temperature estimates from micro- and macrofossil data sets (e.g. Juggins 2013; Brooks & Langdon 2014).

The Last Termination, with its rapid and distinct climate shifts, is an excellent time period to study the nature and regional impact of climate variability. Few lake sedimentary successions in Europe however fulfil the requirement of being chronologically well-constrained, multi-proxy sites that are able to capture the variety of climatic and environmental signals preserved within the fossil record and enable unequivocal comparisons to the Greenland ice core template chronology (Ammann *et al.* 2013; Birks & Birks 2014; Rach *et al.* 2014; Muschitiello & Wohlfarth 2015). One of these is the sedimentary succession from the ancient lake at Hässeldala Port in southern Sweden (Fig 1A-C), which displays a distinct Lateglacial stratigraphy (Davies *et al.* 2004). Since the discovery of several cryptotephra layers in Hässeldala Port's sediments (Davies *et al.* 2003), the site has been the focus of a variety of proxy studies, most of which were performed on various parallel sediment cores (Davies *et al.* 2004; Wohlfarth *et al.* 2006; Watson 2008; Kylander *et al.* 2013; Steinthorsdottir *et al.* 2013, 2014; Ampel *et al.* 2014; Muschitiello *et al.* 2015a, b; Karlatou-Charalampopoulou 2016) (Fig. 1C, Table 1). Except for the most recent studies (Steinthorsdottir *et al.* 2013; Ampel *et al.* 2014; Muschitiello *et al.* 2015b; Karlatou-Charalampopoulou 2016), the chronology of core #2 and visual core-to-core correlations were used (Davies *et al.* 2004; Wohlfarth *et al.* 2006; Watson 2008; Kylander *et al.* 2013). The latter approach was justified because total organic carbon (TOC) and/or loss-on-ignition (LOI) measurements for each analysed profile show the same characteristic pattern and allowed for a direct correlation between parallel sediment cores and their lithostratigraphic units (Wohlfarth *et al.* 2006).

Alignment of the various parallel profiles using a Monte Carlo based approach and the most recent and updated age model for core #5 (Muschitiello

For Review Only

et al. 2015b) now offer the possibility to present the suite of proxy records for Hässeldala Port on one common time scale and to discuss local and regional responses to Last Termination climate events. The different proxies analysed in Hässeldala Port's sedimentary profiles have been described in detail in various publications (see Table 1 for references), but except for the chironomid-based temperature reconstruction and the biomarker data set, which have been presented on an updated chronology (Muschitiello *et al.* 2015a, b), none of the other proxies has been discussed within the context of the new chronology for core #5. Here we combine Hässeldala Port's various sediment cores and proxies and present these on the chronology for core #5 to discuss the timing and impact of Lateglacial climatic shifts in southern Sweden and to address leads and lags between changes in hydroclimate and vegetation across Europe.

Hässeldala Port - background

The ancient lake that existed during the Last Termination at Hässeldala Port (56'16° N, 15'01° E; 63 m a.s.l.) in Blekinge province, southern Sweden (Fig. 1A-C), filled in during the early Holocene. Today the site is a peat bog that is partly covered by a mixed pine-birch forest, shrubs (*Juniperus*, Ericales), grass, mosses and ferns. Peat has been excavated extensively during the first half of the 20th century and Lateglacial sediments can therefore be found in a depth of less than three meters. This, and the easy access to the site, has led to several coring campaigns during the past fifteen years. Coring was always performed using a Russian corer of 1 m length and 10 cm diameter.

Since Hässeldala Port's Lateglacial and early Holocene sediment succession is contained within one meter of sediment, it precisely fits the length of the coring chamber and can be recovered without the need of overlaps. The deepest part of the basin was found to be in the south-western corner of the bog. It is from this restricted area, where all analysed sediment cores have been obtained (Fig. 1C, Table 1). The exact GPS location of each coring point has however not been recorded and lithostratigraphic transects combining all studied profiles are therefore not possible, other than those shown in Wohlfarth *et al.* (2006).

For Review Only

The first to acknowledge the potential of Hässeldala Port's Lateglacial sediments were Davies *et al.* (2003), who described five different cryptotephra horizons from core #1 (Fig. 1C, Tables 1, 2). Of these three were correlated to known eruptions based on their geochemical signatures: the Borrobol tephra (BT), the newly defined Hässeldala tephra (HDT) and the Askja-S tephra (AsT) (Table 2). Two tephras could not be correlated to any known eruption. Using the pattern of the loss-on-ignition (LOI) curve of core #1, Davies *et al.* (2003) tentatively assigned climatic/pollen stratigraphic periods and suggested that the BT would date to the Bølling-Allerød Interstadial and the HDT and the AsT to the early Holocene. However, the finding of two superimposed cryptotephras in Lateglacial sediments in Scotland, which both seem to have been derived from the same volcanic source, led Matthews *et al.* (2011) to suggest that Hässeldala Port's BT is younger than the BT found in Scotland and likely an equivalent to the Penifiler tephra.

Subsequent analyses were made on cores #2 (LOI, ^{14}C chronology) and #3 (TOC, cryptotephra, pollen stratigraphy) (Fig. 1C, Tables 1, 2) (Davies *et al.* 2004; Andersson 2004; Wohlfarth *et al.* 2006). Both profiles showed an identical stratigraphy and a good match between the LOI/TOC curves, which facilitated visual inter-core correlations. The different age models established for core #2 were therefore transferred to core #3 and provided age estimates for the three geochemically identified cryptotephra layers of 14.3-13.7 cal. ka BP ('BT'), 11.6-11.2 cal. ka BP (HDT) and 11.1-10.6 cal. ka BP (AsT) (Wohlfarth *et al.* 2006). The reconstructed vegetation development showed that arctic and sub-arctic plant species dominated during the Lateglacial and that *Pinus sylvestris* and *Betula pubescens* were present at the transition between the Younger Dryas and Preboreal pollen zones (Andersson 2004; Wohlfarth *et al.* 2006). Moreover, approximate ages for the regional Lateglacial pollen zone boundaries were established using a suite of different age models. These suggested ages of 14.2-13.7 cal. ka BP for the Older Dryas/Allerød pollen zone transition, of 13.1-12.6 cal. ka BP for the Allerød/Younger Dryas transition and of 11.9-11.3 cal. ka BP for the Younger Dryas/Preboreal transition (Wohlfarth *et al.* 2006).

A set of twelve new sediment cores were later obtained by Watson (2008), analysed for LOI, cryptotephra, Coleoptera and chironomids (Fig. 1C, Tables 1, 2) and correlated to cores #2 and #3. Six of these profiles were subsampled and aggregated for Coleoptera analysis; LOI analyses were undertaken on four cores to aid cross-core correlation (#HP4, #HP6, #HP9, #HP12) and chironomids were analysed from core #HP4 (Fig. 1C, Table 1). Cryptotephra was found in core #HP4 and was tentatively correlated to core #1 using the pattern of the LOI curve (Watson 2008) (Table 2). The Coleoptera assemblages, which represent mean summer air temperatures, suggested mild and cool summers until about 13.4 cal. ka BP with reconstructed mean summer temperatures of about 14 °C (Watson 2008). At the Younger Dryas/Holocene transition, Coleoptera, which are typical of acid bog environments and dry shrub heathland such as *Amara alpina* and *Olophrum boreale*, appear suggesting a change in lake status. The chironomid assemblages also show clear shifts in species composition and point to a shift from oligotrophic to increasingly eutrophic lake water conditions (Watson 2008). Moreover, the chironomid assemblages allowed reconstructing mean summer surface water temperatures between *c.* 14.2 and 11.8 cal. ka BP in great detail (Watson 2008; Muschitiello *et al.* 2015b).

Kylander *et al.* (2013) analysed the geochemistry in core #4 (Fig. 1C, Table 1) and, using lithostratigraphic markers and the TOC curve, matched this profile to cores #2 and #3 to obtain a general chronostratigraphic framework. Higher sediment accumulation rates were reconstructed for the pre-Allerød period, while a relative constant sediment supply seems to have characterised the Allerød and Younger Dryas pollen zones.

The most recent investigations focussed on core #5 (Fig. 1C) and provided a new chronology and age model, an atmospheric CO_2 reconstruction using leaf stomata (Steinthorsdottir *et al.* 2013, 2014), lake status changes based on diatom assemblages (Ampel *et al.* 2014) and geochemistry (Muschitiello *et al.* 2015a) and a hydroclimate reconstruction using lipid biomarkers (Muschitiello *et al.* 2015b). These latter analyses were based on hydrogen isotopes derived from aquatic (n-C_{21}) and terrestrial (n-$C_{27\text{-}29\text{-}31}$) alkanes and can be used as proxies for moisture source composition and terrestrial evaporation (Muschitiello *et al.* 2015b) (Table 1). All sub-samples were taken in 1 cm increments along core #5 and split to accommodate various proxy analyses.

However, to provide enough leaf material for stomatal analyses, several parallel cores had to be sub-sampled after precise lithostratigraphic correlation to the master core #5 (Steinthorsdottir *et al.* 2013, 2014). Lastly, a new high-resolution pollen stratigraphy, combined with LOI measurements, was established on parts of core #6 (Muschitiello *et al.* 2015b; Karlatou-Charalampopoulou 2016) (Fig. 1C, Table 1).

Although the lithostratigraphy and the LOI/TOC curves for the parallel profiles facilitated visual core-to-core correlations (Wohlfarth *et al.* 2006), this eyeballing exercise did not allow for a precise transfer of proxy data from one core to another. Muschitiello *et al.* (2015b) therefore statistically aligned cores #2, #HP4, #5 and #6 with each other. This made it possible to update the existing chronology for core #5 and provided a possibility to discuss climate responses across the Allerød/Younger Dryas pollen zone transition in greater detail (Muschitiello *et al.* 2015b).

Lithostratigraphy and core-to-core correlations

Hässeldala Port's sediment cores are all derived from the southwestern part of the peatbog (Fig. 1C) and display an almost identical lithostratigraphic succession, which is also reflected in the respective TOC/LOI curves (Davies *et al.* 2003, 2004; Wohlfarth *et al.* 2006; Kylander *et al.* 2013; Steinthorsdottir *et al.* 2013, 2014; Karlatou-Charalampopoulou 2016). Since the bottom topography of the bog is not even, the depth of the Lateglacial/early Holocene profiles varies slightly, as does the thickness of individual layers (Wohlfarth *et al.* 2006) (Figs 2, 3A). Despite this, the recovered Lateglacial/early Holocene successions show a distinct and repetitive lithostratigraphic pattern (Figs 2, 3A): the bottommost sediments in all cores are composed of grey silty sand and clayey silt/silty clay (units 1 and 2) with low organic matter content; higher, but variable LOI/TOC values characterise the silty clay gyttja and/or clay gyttja layers of units 3 to 6 (Fig. 2); and the dark brown silty clayey gyttja/clayey gyttja of unit 7 with its high LOI/TOC values is distinct in all profiles, as is the overlying greenish-brown/brown clayey gyttja of unit 8 with its markedly lower LOI/TOC values

For Review Only

(Wohlfarth *et al.* 2006) (Fig. 2). The sediments in the uppermost part are made up of clay gyttja, gyttja and peaty gyttja (units 9-12) with high LOI/TOC values.

Lithostratigraphic core-to-core correlations are thus straightforward and are also supported by the very similar pattern of the accompanying LOI/TOC curves (Figs 2, 3A). These display the same characteristic features in all six sequences with low organic contents in the bottommost part, gradually rising, but variable TOC/LOI values, a distinct peak in organic content, a decrease in LOI/TOC values and subsequent high values (Fig. 3A). However visual core-to-core correlations or visual curve matching do not allow transferring proxies from one sediment core to another or projecting the various proxies on the new chronology of core #5. We therefore follow the approach presented in Muschitiello *et al.* (2015a, b), who used a Monte Carlo Markov Chain algorithm for core-to-core alignment. This method provides a suite of possible alignments between stratigraphic series and the target series and estimates the optimal correlation (see Muschitiello *et al.* 2015b for further details). For Hässeldala Port, we use the high-resolution LOI/TOC curves of cores #1-3, HP4 and 6 as stratigraphic series and the LOI curve of core #5 as target series (Fig. 3A). Prior to the statistical analyses, the TOC values of cores #1, 2 and 3 were recalculated to LOI values to facilitate the statistical correlation. The alignment of the LOI curves of cores #1-3, HP4 and 6 to the LOI curve of core #5 then provided a means to transfer the plant macrofossil record and the ^{14}C dates of core #2, the pollen stratigraphy of core #3 (Wohlfarth *et al.* 2006), the chironomid-based summer temperature reconstruction of core #HP4 (Watson 2008) and the high-resolution pollen stratigraphy of core #6 (Karlatou-Charalampopoulou 2016) to the stratigraphy of core #5 (Muschitiello *et al.* 2015b). However, since the chironomid data set of core #HP4 had a higher temporal sampling resolution than samples taken from core #5, the data set had to be interpolated to the sampling resolution of master core #5 (Muschitiello *et al.* 2015b).

Age-depth model and chronology

Using the same core-to-core alignment approach as outlined above, Muschitiello

For Review Only

et al. (2015b) updated the earlier age model for core #5 (Steinthorsdottir *et al.* 2013, 2014) by transferring the ^{14}C dates from core #2 to the stratigraphy of core #5 (Table 3, Fig. 4).

Age-depth curves were constructed (Muschitiello *et al.* 2015b) using Bacon2.2. (Blaauw & Christen 2011) and OxCal4.2 (Bronk Ramsey 2010) after calibration with IntCal13 (Reimer *et al.* 2013). Since both age models provided very similar results, we here use OxCal4.2 modelled weighed mean ages for the respective age-depth assignments (Table 4). Parts of the uppermost and/or lowermost layers in some profiles do not overlap with the length of core #5. The chronology for these parts had therefore to be estimated using the modelled sedimentation rate of the respective lithostratigraphic units (Fig. 3B, Table 4). The new composite age model for core #5 (Muschitiello *et al.* 2015b) compares well with the previous age model (Steinthorsdottir *et al.* 2013, 2014) in terms of shape of the age-depth relationship and age output values. It however provides a higher number of time constraints, especially between 13 and 11 cal. ka BP (Muschitiello *et al.* 2015b).

When plotted on the new time scale of core #5, the main features of the six LOI/TOC curves fall within the same time interval, such as the decrease in LOI/TOC values at 13 cal. ka BP, their peak between 12.8 and 12.7 cal. ka BP, as well as the mid-point of their gradual rise at 11.5 cal. ka BP (Fig. 3B). Moreover, modelled ages differ by less than 150 years for both the 'Borrobol' and Askja-S tephra and by less than 50 years for the Hässeldala tephra between cores #1 and 3 (Fig. 3B). The good temporal correspondence of the main features in the six sediment cores gives confidence in the statistical curve alignments and provides a new chronological basis for discussing the Lateglacial environmental and climatic history of southern Sweden.

Local and regional environmental and climatic development

>14.1 cal. ka BP

Glacial varve chronologies, glacial stratigraphy and geomorphology, and pollen stratigraphic studies in Blekinge province, southernmost Sweden, reconstruct a rapid decay of the Scandinavian Ice Sheet margin in response to the temperature

For Review Only

rise at the start of the Bølling-Allerød interstadial at 14.7 cal. ka BP (Björck & Möller 1987; Ringberg 1991; Wohlfarth *et al.* 1994; Lundqvist & Wohlfarth 2001; Anjar *et al.* 2013). The combination of ice sheet load, ice sheet melt and isostasy created a large ice lake in the Baltic Sea basin (Björck 1995; Andrén *et al.* 2011), whose highest shoreline reached up to ~65-67 m a.s.l. in Blekinge (Björck 1981; Ringberg 1991).

The local glacial varve chronology shows that coastal areas in southern Blekinge had become free of active ice within 100 years (Fig. 5A) and that the formation of the highest coastline at 65-67 m a.s.l. likely corresponds to an ice marginal position at around local varve year 0 (Ringberg 1991). Rapid land uplift followed coastal deglaciation and led to an apparent lowering of the Baltic Ice Lake shoreline (Björck 1981; Wohlfarth *et al.* 1994). The deposition of exceptionally thick varves, which can be seen in many clay-varve diagrams from Blekinge (corresponding to local varve years +88 to +220) (Ringberg 1991; Wohlfarth *et al.* 1994), signals accelerated ice sheet melt and likely correlates to fluvio-glacial delta surfaces at around 55 m a.s.l. (Björck 1981). More or less coinciding with the appearance of the thick varves, the area around Hässeldala Port became free of active ice, as seen in the deglaciation ages for sites such as Trehörnan, Hemsjön, Kroksjön II and Skälgylet (Fig. 5B, Table 5). Glacial varves did however not form at Hässeldala Port since the site was located at much shallower depths and close to the shoreline of the Baltic Ice Lake (Fig. 5C). Pollen stratigraphic studies of the varved-clay succession of Farslycke (Ising, 1998) and Kroksjön II (Björck 1981) (Fig. 5B) and plant macrofossil finds of *Salix polaris*, *S. reticulata*, *S. herbacea*, *Dryas octopetala*, and *Betula nana* in the thick varves (Wohlfarth *et al.* 1994) suggest that herb and shrub vegetation had become established on ice-free land areas. Pollen assemblages (Farslycke, Kroksjön) and ^{14}C ages on terrestrial plant remains (Farslycke, Skälgylet) assign the thick varves to the Bølling pollen zone (Björck 1981, 1984; Björck & Möller 1987; Ising 1998; Wohlfarth & Possnert 2000; Lundqvist & Wohlfarth 2001). Varves assigned to local varve years +220 to +360 become gradually thinner displaying a greater distance to the rapidly melting ice sheet margin, which was now located some 50-100 km to the north of Blekinge's present coastline, and drained by large overland rivers (Björck & Möller 1987; Möller 1987). Lake isolation

For Review Only

studies, combined with pollen stratigraphies, show that land uplift was still rapid and that the shoreline of the Baltic Ice Lake was successively lowered to around 50-55 m a.s.l. at the end of the regional Bølling pollen zone (Figs 5B, C) and to around 45-50 m a.s.l. (Fig. 5D) at the end of the regional Older Dryas pollen zone (Björck 1981, 1984).

The gradual emergence of new land areas meant that Hässeldala Port's location changed from an archipelago setting during the Bølling pollen zone to further inland during the Older Dryas pollen zone (Figs 5C, D). The bottommost silty fine sand (unit 1) in Hässeldala Port's successions (Figs 2, 6A) could derive from melting of stagnant ice or run-off from poorly vegetated slopes. Coleoptera assemblages suggest mild and cool summers during this early period with mean summer air temperatures of about 14 °C (Watson 2008) and the presence of *Hippophaë rhamnoides* and *Nymphaea alba* in the aquatic pollen record of Hässeldala Port (Andersson 2004) indicates minimum mean July temperatures of >10 °C and possibly as much as 11-12 °C (Iversen, 1954; Kolstrup 1980). In contrast, mean July surface water temperatures reconstructed from chironomid assemblages are around 7-8 °C (Fig. 6E) and may represent a lake water temperature that was strongly influenced by run-off from stagnant ice. The herb, grass, shrub and dwarf-shrub dominated pollen assemblages (HÄP-1) (Andersson 2004; Wohlfarth *et al.* 2006) suggest that these lowermost sediments were deposited during the regional Older Dryas pollen zone (Figs 6H, J).

Plant macrofossil finds and pollen stratigraphic records in Blekinge dating to the regional Older Dryas pollen zone (Berglund 1966; Björck 1981; Wohlfarth *et al.* 1994, 2006) reveal a shrub-grass-herb vegetation, that comprised *Artemisia, Betula nana*, *Calluna vulgaris*, *Caltha palustris*, *Dryas octopetala*, *Empetrum nigrum*, *Ephedra*, *Helianthemum*, *Hippophaë rhamnoides*, *Juniperus communis*, *Plantago*, *Polygonum*, *Rumex*, *Saxifraga*, *Salix polaris*, and *Urtica* (Table 6). Pollen of *Populus tremula* (Berglund 1966) and plant macrofossil finds of *Betula pubescens* (Wohlfarth *et al.* 1994) (Table 6) moreover point to the regional presence of shrub-like trees. Regional minimum mean July temperatures of >10 °C for *Betula pubescens* (Iversen 1954) compare well to those inferred from Coleoptera species and pollen in Hässeldala's sediments.

For Review Only

14.1 – 12.7 cal. ka BP

Hässeldala's silty clay, gyttja clay and clayey gyttja (units 2 – 7) and the accompanying LOI curve demonstrate a gradually higher organic matter content of the sediments, but also that minerogenic inputs still dominate (Figs 6A, B). LOI displays a first marked increase at 13.7 cal ka BP, coinciding with the start of unit 3, and thereafter fluctuates between lower (13.5-13.4 cal. ka BP; 13.05-12.95 cal. ka BP) and higher values (13.7-13.55 cal. ka BP; 13.3-13.1 cal. ka BP; 12.9-12.7 cal. ka BP) (Fig. 6B). Accumulation rates seem to have been rather stable throughout this time interval, except for around 14.1-13.7 and 13.0-12.9 cal. ka BP, when sediment accumulation was slightly higher (Kylander *et al.* 2013).

The tephra layer that had been assigned to the Borrobol tephra (Davies *et al.* 2003, 2004; Wohlfarth *et al.* 2006) (Fig. 6F), but has been discussed as being an equivalent of the Penifiler tephra (Mathews *et al.* 2011) falls within the interval of low LOI values. The core-to-core alignment and the new chronology for core #5 suggest that this tephra layer dates to around 14.1-13.7 cal. ka BP.

In conjunction with the increase in LOI values at 13.7 cal. ka BP (Fig. 6B), diatom-inferred lake water pH shifts to more acid values (Fig. 6C). This distinct shift could be the result of increased surface flow that transported organic acids from surrounding soils into the shallow lake (Ampel *et al.* 2014) and could indicate that the catchment vegetation had become denser. Lake waters become neutral around 13.5 cal. ka BP and remain, apart from a few minor fluctuations, around a pH of 7 until 12.7 cal. ka BP (Fig. 6C). The diatom assemblages and the crysophyte:diatom ratios (C:D) in the lowermost diatom zone (DAZ-I; 14.1-13.2 cal. ka BP) (Fig. 6C) suggest cold lake water conditions, low light and nutrient availability, but also a gradual shortening of the ice-covered season (Ampel *et al.* 2014). Leaf-wax derived hydrogen isotopes, δD_{n}-C_{21} and $\Delta\delta D_{terr\text{-}aq}$, which reflect the isotopic composition of the source moisture and terrestrial evaporation, respectively indicate a saline moisture source and minor shifts between drier and wetter conditions (Fig. 6D). However the measurement errors are too large to render these values significant. Chironomid-derived mean July surface water temperatures show a step-wise increase from 8 °C at 14.1 cal. ka BP to maximum

For Review Only

values of 12-13 °C at 13.2-13.1 cal. ka BP (Fig. 6E). Coleoptera assemblages are still composed of species typical of cool and mild climates, but reconstructed summer temperatures now reach >14 °C (Watson 2008) and seem to be comparable to chironomid-inferred temperatures.

The Hässeldala Port proxies suggest marked changes between 13.2 and 12.7 cal. ka BP. In diatom zone DAZ-II (13.2-12.6 cal. ka BP) (Fig. 6C) the habitat structure in the shallow lake changes, open water taxa decline, but the diatom flora becomes more diverse and attached-growing species become more abundant. This points to denser aquatic vegetation, possibly in response to a lake level lowering and/or higher nutrient availability (Ampel *et al.* 2014). The C:D ratio shows a decline in the number of crysophyte cysts relative to diatoms, which points to a shorter ice-covered season (Fig. 6C). $\delta D_{n\text{-}C_{21}}$ values start to decrease at 13.2 cal. ka BP and reach minimum values between 13.0-12.8 cal. ka BP, coincident with higher $\Delta\delta D_{terr\text{-}aq}$ values (Fig. 6G). This shift in hydrogen isotope values suggests a freshening of the marine moisture source region and distinctly drier conditions at Hässeldala Port (Muschitiello *et al.* 2015b). The trend of decreasing $\delta D_{n\text{-}C_{21}}$ values and increasing $\Delta\delta D_{terr\text{-}aq}$ values was shortly interrupted at 12.7 cal. ka BP, when more saline moisture reached the site and conditions became wetter. The observed two-step decrease in δD_{aq} values (13.0-12.8 and after 12.7 cal. ka BP) has been interpreted as a progressive freshening of the Atlantic precipitation water source for Hässeldala Port caused by the melting of the Fennoscandian Ice Sheet (Muschitiello *et al.* 2015b). The distinct shift in hydrogen isotope values and diatom assemblages around 13.2 cal. ka BP coincides with a decline in mean July surface water temperatures to around 10-11 °C (Fig. 6C-E).

The main features in local pollen assemblage zones HÄP-2 (14.1-13.2 cal. ka BP) (rise in *Juniperus communis* pollen percentages) and HÄP-3 (13.2-12.7 cal. ka BP) (increase in *Empetrum* and Ericales pollen values) (Andersson 2004; Wohlfarth *et al.* 2006) allow for a correlation to the regional Allerød I and II pollen zones (Björck & Möller 1987), respectively (Fig. 6H, J). *Nymphaea alba* pollen are continuously present in low numbers in HÄP-2 and HÄP-3 (Andersson 2004) and thus suggest that minimum mean July temperatures were >10 °C (Kolstrup 1980). HÄP-3 correlates to local pollen zone Hä-1 and to parts of local

For Review Only

pollen zone Hä-2, which were recently established on core #6 (Karlatou-Charampopoulou 2016) (Fig. 6I) and detail the vegetation changes that occurred at the regional Allerød/Younger Dryas transition (see below).

Pollen stratigraphic data sets for Blekinge (Berglund 1966; Björck & Möller 1987) show that herbs and shrubs still dominate, but that the regional vegetation had become more diverse. Plant species now also include *Astralagus alpinus, Cerstium alpinum, Dryopteris, Isoëtes, Jasione montana, Lycopodium, Lastrea, Myriophyllum alterniflorum, Populus tremula, Potentilla palustris, Prunus padus, Pimpinella, Polypodium, Ranunculus, Rubus, Sanguisorba, Sorbus, Typha latifolia* and *Valeriana officinalis* (Berglund 1966) (Table 6). Moreover, plant macro-remains of *Betula pubescens* have been reported (Berglund 1966).

Minimum mean summer temperatures based on indicator species, such as *Betula pubescens* (Iversen 1954), *Hippophaë rhamnoides, Typha latifolia* (Kolstrup 1980), and *Jasione montana* (Kolstrup 1979) (Table 6), suggest that minimum mean July temperatures were around 12-15 °C. However these values relate to the whole of the regional Allerød pollen zone and do not allow any differentiation of changes through time. The chironomid-based summer surface water temperature reconstruction and the age model for Hässeldala Port now provide a more detailed view of the temperature evolution between 14.1 and 12.7 cal. ka BP and indicate that warm mean July temperatures were only attained between 13.4-13.1 cal. ka BP (Fig. 6E).

The increase in organic matter content seen in Hässeldala Port's sediments between 12.9-12.7 cal. ka BP (Figs 3A, 6B) is a feature that is typical for many Lateglacial sequences in southern Sweden (Björck & Möller 1987; Berglund *et al.* 1994). It has been long argued that this increase represents the in-wash of topsoil material that was released during the final melting of remnant ice or could indicate a lake level lowering due to drier climatic conditions (Digerfeldt 1971). A C/N ratio of 13 and bulk δ^{13}C values of around -18‰ for Hässeldala Port do not support increased in-wash of terrestrial organic material, but rather point to a dominance of aquatic sourced organic matter (Kylander *et al.* 2013). Moreover, higher $\Delta\delta D_{terr\text{-}aq}$ values and lower mean July temperatures that coincide with the peak in LOI indicate drier and slightly colder conditions (Figs 6D, E), which could have led to a lake level lowering. This scenario

For Review Only

compares well with the findings of Ampel *et al.* (2014), who had suggested a lowering of the lake level as a result of drier conditions. A lower lake level and expansion of the aquatic vegetation could have raised the nutrient level in the already shallow lake as reflected by high LOI values.

12.7-11.8 cal. ka BP

The lithological boundary between the dark brown clayey gyttja (unit 7) and the greenish-brown/brown clayey gyttja (unit 8) is reflected by a decrease in LOI values (Figs 6A, B). LOI values remain low until *c.* 11.8 cal. ka BP and gradually increase thereafter (Fig. 6B). This increase is coupled to a change in sediment colour and lithology (unit 9). The initial decrease and later increase in lake organic productivity is mirrored by geochemical proxies (Kylander *et al.* 2013), which suggest relatively stable conditions between 12.7 and 12.0 cal. ka BP, but changes in source material and/or hydrology and in aquatic productivity thereafter.

Opportunistic diatom taxa (e.g. *Staurosirella pinnata*), which compete well under challenging environmental conditions, increase in abundance in diatom zone DAZ-III (12.6-11.8 cal. ka BP), as do the relative numbers of chrysophyte cysts (12.6-12.3 cal. ka BP) (Ampel *et al.* 2014) (Fig. 6C). The increase in crysophyte cysts suggests that nutrient levels had decreased, which would be in line with lower lake organic productivity as inferred by lower LOI values (Fig. 6B). This change in lake status (low nutrient, low productivity) together with colder temperatures and longer ice-cover seasons gave certain diatom species an advantage (Ampel *et al.* 2014).

The decline in mean July surface water temperatures, which starts at 12.7 cal. ka BP, continues until 12.5-12.4 cal. ka BP, when the lowest reconstructed temperatures of 8 °C are reached (Fig. 6E). Coincident with the decline in temperatures, $\delta D_{n\text{-}C_{21}}$ values decrease and $\Delta\delta D_{terr\text{-}aq}$ values increase, suggesting a fresher moisture source and progressively drier conditions (Fig. 6D). Mean July surface water temperatures fluctuate and stay around 9-10 °C between 12.4-11.9 cal. ka BP, but subsequently start rising again from 9 °C to 12 °C (Fig. 6E). This steady rise more or less coincides with distinct changes in $\delta D_{n\text{-}C_{21}}$ and $\Delta\delta D_{terr\text{-}aq}$

For Review Only

values (Fig. 6D), which show a shift towards a more saline marine moisture source of precipitation and wetter conditions around 11.8 cal. ka BP (Muschitiello *et al.* 2015b).

The decrease in *Empetrum* pollen values and the increase in herb and grass pollen percentages, especially for *Artemisia*, defines local pollen zone HÄP-4 (Andersson 2004; Wohlfarth *et al.* 2006) (12.7-11.7 cal. ka BP). This local pollen zone, which partly overlaps with local pollen zones Hä-3, Hä-4 and Hä-5 on core #6 (Karlatou-Charalampopoulou 2016), was correlated to the regional Younger Dryas pollen zone (Figs 6H-J) of Berglund (1966) and Björck & Möller (1987) (Andersson 2004; Wohlfarth *et al.* 2006) (see below). *Nymphaea alba* pollen, which are present during HÄP-4 (Andersson 2004) suggest minimum mean July temperatures of >10 °C (Kolstrup 1980), which compares to those reconstructed from chironomid assemblages (Fig. 6E).

Pollen stratigraphies for Blekinge (Berglund 1966; Björck & Möller 1987) show that the expanding herb and shrub vegetation comprised *Artemisia, Astralagus alpinus, Betula nana, Calluna vulgaris, Cerastium alpinum, Chamaenerion alpinum, Dryas octopetala, Dryopteris, Empetrum nigrum, Ephedra, Helianthemum, Hippophaë, Jasione montana, Juniperus communis, Lycopus europaeus, Minuartia, Myriophyllum alterniflorum, M. spicatum, M. verticillatum, Oxytropis capestris, Oxyria digyna, Plantago, Polygonum, Potentilla palustris, Populus tremula, Ranunculus, Rumex acetosella, Rubus, Sanguisorba, Sorbus, Saxifraga, Selaginella selaginoides,* and *Urtica* (Table 6). Interestingly, also *Pinus sylvestris* macrofossil remains have been reported for this time interval (Berglund 1966). This is surprising given that these had not been found during the Allerød pollen zone. On the other hand, especially high pollen values for *Pinus* in Allerød lake sediments in Blekinge could be an indication for the presence of these trees prior to the regional Younger Dryas pollen zone (Björck 1979). *Pinus* may have thus survived in micro-climatically favourable habitats or the macrofossil finds of *Pinus sylvestris* relate to the very end of the regional Younger Dryas pollen zone.

Plant indicator species (Table 6), such as *Hippophaë rhamnoides, Myriophyllum alterniflorum, M. spicatum, M. verticillatum* and *Jasione montana,* would suggest that minimum mean summer temperatures reached 10-12 °C

For Review Only

(Kolstrup 1979; 1980). These values however relate to the regional Younger Dryas pollen zone in general and do not allow differentiation of changes through time. The chironomid-based temperature reconstruction for Hässeldala Port shows that mean July surface water temperatures fluctuated between 8-10 °C during the Younger Dryas and rose to >10 °C only at 11.9 cal. ka BP (Fig. 6E). Since *Pinus sylvestris* requires minimum mean summer temperatures of >12 °C (Iversen 1954), we speculate that the macrofossil finds reported by Berglund (1966) stem from the latest part of the regional Younger Dryas pollen zone, when summer temperatures had already increased.

In and out of the Younger Dryas pollen zone

It is interesting to look closer into the sequence of events around the start and end of the regional Younger Dryas pollen zone since several of Hässeldala Port's proxies (LOI, hydrogen isotopes and diatom assemblages) have been analysed on the same split samples of core #5. The chironomid-derived temperature reconstruction and the pollen stratigraphies were however established on parallel cores that were aligned to the chronology of core #5 using the approach of Muschitiello *et al.* (2015b). The former therefore allow for a direct comparison, independent of the age assignment, while minor time lags detected for the latter could be an artefact because age model errors are not taken into account here.

The most recent pollen stratigraphy for Hässeldala defines local pollen zone Hä-2 (12.77-12.54 cal. ka BP) as a transition zone between the regional Allerød and Younger Dryas pollen zones (Figs 6I, J) (Karlatou-Charalampopoulou 2016). This pollen zone is characterised by a first increase in *Artemisia* pollen values and a decrease in pollen concentrations. These changes seem to have occurred more or less coincident with several other proxies. Sediment organic matter content declines, the number of crystophyte cysts over diatoms starts to increase (Fig. 6C), hydrogen isotope proxies show a brief return to wetter conditions at *c.* 12.7 cal. ka BP that was followed by progressively drier conditions (Fig. 6D) and chironomid-inferred summer surface lake water temperatures decline (Fig. 6E). Slight differences between the lower boundaries

For Review Only

of HÄP-4 and Hä-3 are due to how pollen zones transitions were originally defined, as the increase in *Artemisia* pollen values in core #3, which is comparable to the lower boundary of Hä-3, actually already occurs at 12.7 cal. ka BP (Andersson 2004).

Hä-5 (11.85-11.58 cal. ka BP) reflects the transition zone between the regional Younger Dryas and Preboral pollen zones (Figs 6I, J) and is defined by decreasing *Juniperus* and *Artemisia* pollen percentages and rising *Empetrum* pollen values (Karlatou-Charalampopoulou 2016). The start of Hä-5 predates the transition between pollen zones HÄP-4 and HÄP-5 (11.7 cal. ka BP), but coincides with rising sediment organic matter content, changes in diatom assemblages, marked shifts in hydrogen isotope values and a rise in chironomid-inferred summer surface water temperatures (Fig. 6B-I).

Hässeldala Port's proxies thus provide no clear evidence for distinct local lags in response to regional climatic changes at the start and end of the Younger Dryas. Minor divergences, as seen in the comparison between the two pollen stratigraphic records (Fig. 6H, I), are an artefact of where and how pollen zone boundaries are drawn and defined.

11.8-10 cal. ka BP

Hässeldala Port's sediments shift from clayey gyttja (unit 8) to gyttja (units 9-11) around 11.8 cal. ka BP and to peaty gyttja (unit 12) at 10.9 cal. ka BP (Fig. 6A). The steady increase in LOI values and subsequent values of >80% depict the increase in sediment organic matter and show that the small lake gradually filled in (Fig. 6B). This is also reflected in the diatom assemblages of DAZ-IV, which suggest a transition towards a less alkaline mire environment that gradually turned into a rather dry mire environment (Ampel *et al.* 2014). Coleoptera, which are typical of acid bog environments and dry shrub heathland, such as *Amara alpina* and *Olophrum boreale* now appear (Watson 2008). The trend to overall wetter conditions as seen in decreasing $\Delta\delta D_{terr-aq}$ values was briefly interrupted around 11.5 cal. ka BP, when hydrogen isotope values suggest both a freshening of the marine sources of precipitation and a return to slightly drier conditions (Fig. 6D). The timing of this shift compares to the Preboreal

Oscillation, a short cooling phase identified in North Atlantic paleo-records (Björck *et al.* 1996, 1997) and predates the oscillation discussed earlier by Wohlfarth *et al.* (2006) based on the LOI curve of core #3. The Hässeldala tephra, identified in core #1 and 3 (Davies *et al.* 2003, 2004; Wohlfarth *et al.* 2006), occurs around 11.3 cal. ka BP and thus after the oscillation seen in the hydrogen isotope proxies (Fig. 6D, F). Cryptotephra, which has been geochemically assigned to the Askja-S tephra was also found in cores #1 and 3 and can now be dated to around 10.9-10.7 cal. ka BP (Fig. 6F).

Local pollen zone HÄP-5 (11.7-11.3 cal. ka BP) (Andersson 2006) overlaps with local pollen zones Hä-5 and Hä-6 in core #6 (11.85-11.3 cal. ka BP) (Karlatou-Charalampopoulou 2016) (Fig. 6H, I). The distinct peak in *Empetrum* pollen percentages, a decrease in *Artemisia* pollen values and overall a slight increase in tree pollen, mainly of *Betula*, allows correlations to the YD-PB transition zone of Berglund (1966) and Björck & Möller (1987). The YD-PB transition zone has been assigned to the early part of the regional Preboreal pollen zone (Björck *et al.* 1996), thus marking the start of the Holocene. Macroscopic charcoal appears in large quantities around 11.8-11.6 cal. ka BP and the first macroscopic finds of *Betula pubescens* occur at 11.6-11.4 cal. ka BP (Wohlfarth *et al.* 2006) (Fig. 6G). Tree pollen percentages increase further in HÄP-6 (11.3-10.9 cal. ka BP) and HÄP-7 (10.9-10.3 cal. ka BP), herb and shrub pollen decline (Andersson 2006), and the presence of *Pinus sylvestris* is attested by finds of needles at 11.0 cal. ka BP (Wohlfarth *et al.* 2006) (Fig. 6G, H). Aquatic pollen of *Typha angustifolia* and *Nymphaea alba* in HÄP-6 and of *Myriophyllum alterniflorum/spicatum* in HÄP-7 (Andersson 2004) suggest that minimum July temperatures had increased distinctly and may have reached >14 °C (Kolstrup 1980). Wetter conditions, as suggested by decreasing $\Delta\delta D_{terr\text{-}aq}$ values (Fig. 6D), and warmer summers likely favoured the further establishment and expansion of trees in Hässeldala Port's catchment. HÄP-6 and HÄP-7 are correlated to the regional Preboreal pollen zones of Berglund (1966).

The vegetation during the regional early Preboreal pollen zone in Blekinge now also included *Botumus umbellatus*, *Caltha palustris, Isoëtes lacustris, Littorella uniflora, Menyanthes trifoliata, Rubus fruticosus,* and *Typha latifolia,* and *Pinus sylvestris* (Berglund, 1966) (Table 6). This latter species, as well as the presence of *Typha latifolia* and *Betula pubescens*, in addition to other indicator species, suggests that minimum mean July temperatures now reached >12 °C (Iversen 1954; Kolstrup 1980). This assumption compares nicely to higher summer temperatures inferred from chironomid assemblages (Fig. 6E) and aquatic pollen.

Wider implications

Hässeldala Port's pollen-stratigraphic records of cores #3 (Andersson 2004; Wohlfarth *et al.* 2006) and #6 (Karlatou-Charampopoulou 2016) and the refined age model now provide a new chronological template for Lateglacial climatic and environmental changes in southern Sweden (Table 7). Andersson's (2004) HÄP-1, which is correlated to the regional Older Dryas pollen zone, is dated to >14.06 cal. ka BP. HÄP-2 compares to the regional Allerød I pollen zone and ranges between 14.06 and 13.24 cal. ka BP and HÄP-3 or the regional Allerød II pollen zone dates to between 13.24 and 12.67 cal. ka BP. Wohlfarth *et al.* (2006) had earlier correlated local pollen zone HÄP-4 (12.67-11.68 cal. ka BP) with the regional Younger Dryas pollen zone, but this correlation now needs to be revised, following the high-resolution pollen stratigraphy of core #6 (Karlatou-Charampopoulou 2016). This latter work shows that a Late Allerød/early Younger Dryas transition zone (Hä-2: 12.77-12.54 cal. ka BP) overlaps with parts of Andersson's (2004) pollen zones HÄP-3 and HÄP-4 (Fig. 6I, J) and suggests that changes in vegetation composition already commenced at 12.77 cal. ka BP (Table 7). Karlatou-Charampopoulou's (2016) local pollen zones Hä-3 and Hä-4 correlate to the regional Younger Dryas pollen zone as defined by Björck & Möller (1987) and extend between 12.54 and 11.85 cal. ka BP (Table 7). The transition between the regional Younger Dryas and Preboreal pollen zones (Berglund 1966; Björck & Möller 1987), which Björck *et al.* (1996) had assigned to the early Holocene, is also clearly seen in Hässeldala Port's pollen stratigraphy. It is represented by pollen zone Hä-5 (Karlatou-Charampopoulou 2016) (Fig. 6 I, J) and dated to 11.85-11.58 cal. ka BP (Table 7).

For Review Only

Muschitiello & Wohlfarth (2015) earlier discussed the time-transgressive nature of vegetation changes in northern Europe around the Allerød – Younger Dryas transition using well-dated pollen stratigraphic records. They showed that the early response seen in Sluggan Bog, Northern Ireland (Walker *et al.* 2012) (13.0 cal. ka BP) predates vegetation shifts in sites located further to the east by *c.* 300-350 years (Fig. 7) and hypothesize that this may have been caused by regional cooling around the Nordic Seas. Hässeldala Port now adds an important data point to this network and supports Muschitiello & Wohlfarth's (2015) conclusions that vegetation shifts reconstructed for sites in Norway, Sweden and western Germany postdate those in Northern Ireland and also occurred 100-250 years later than the onset of Greenland Stadial 1 (Fig. 7). The change in vegetation composition seen in Kråkenes (Norway) at 12.75-12.7 cal. ka BP (Birks *et al.* 2000), Madtjärn (Swedish west coast) at 12.7-12.6 cal. ka BP (Björck *et al.* 1996), Hässeldala Port between 12.77-12.54 cal. ka BP and in Meerfelder Maar (Germany) at 12.7-12.65 cal. ka BP (Rach *et al.* 2014) thus only took place at a time when critical threshold temperatures had been reached and when Greenland ice cores reflect the establishment of full stadial climate conditions and a stadial atmospheric circulation regime (Steffensen *et al.* 2008; Rach *et al.* 2014; Muschitiello & Wohlfarth 2015).

This hypothesis can be tested by comparing the timing of hydroclimate shifts and vegetation records using the two available detailed δD stratigraphies of Hässeldala Port (Muschitiello *et al.* 2015b) and Meerfelder Maar (Rach *et al.* 2014). The δD_{aq} records from Hässeldala Port and Meerfelder Maar show a consistent trend towards more negative values at the start of the Younger Dryas pollen zone (Fig. 8). This suggests large-scale cooling and more negative δD values of the marine moisture source of precipitation – the North Atlantic Ocean – associated with a southward diversion of the storm track trajectories and sea-ice expansion (Rach *et al.* 2014). More interestingly, the two records display an opposite hydro-climate behaviour between southern Sweden and western Germany during the Late Allerød pollen zone/Greenland Interstadial 1a (*c.* 13.1-12.9 cal. ka BP), with relatively lower δD_{aq} values at Hässeldala Port and relatively higher δD_{aq} values at Meerfelder Maar. This pattern is also evident in the $\Delta\delta D_{terr\text{-}aq}$ profiles, which suggest drier conditions at Hässeldala Port as opposed to more humid conditions at Meerfelder Maar (Fig. 8). Muschitiello *et al.* (2015b) suggested that such opposite hydro-climate patterns prior to the start of the Younger Dryas are an expression of increased freshwater forcing from the Fennoscandian Ice Sheet to the Nordic Seas, which affected the hydro-climate system at synoptic scale. Climate model simulations indeed show that freshwater forcing from the Fennoscandian Ice Sheet results in relatively lower atmospheric pressure over the western sector of Europe and Greenland, whereas Northern Europe is affected by relatively higher-pressure conditions (Muschitiello *et al.* 2015b). This scenario could explain the spatially complex differences in moisture availability across the North Atlantic (Muschitiello *et al.* 2015b). The hydro-climate records from Hässeldala Port and Meerfelder Maar also show that southern Sweden likely experienced drier conditions as compared to Western Europe during the Younger Dryas (Fig. 8). This is in line with evidence of increasing continentality and more severe aridity in Europe from south to north (e.g. Birks *et al.* 2014).

The transition out of the Younger Dryas is equally interesting. At *c.* 11.9 cal. ka BP, δD_{aq} values from Hässeldala Port and Meerfelder Maar start to rise and increase by ~40‰ and 30‰, respectively (Fig. 8). The shifts in δD_{aq} are paralleled by changes in $\Delta\delta D_{terr\text{-}aq}$, which indicate progressively wetter conditions both in Western Germany and southern Sweden (Fig. 8). Moreover, these hydro-climate shifts were initiated *c.* 300 years earlier in Europe than the transition into the Holocene in Greenland (Fig. 8). This sequence of events is in agreement with the hypothesis of a gradual northward recession of the North Atlantic sea-ice margin during the second half of the Younger Dryas, which paved the way for a strengthening of the Atlantic Meridional Overturning Circulation associated with the start of the warm Holocene interglacial (e.g. Lane *et al.* 2013; Pearce *et al.* 2013; Bartolomé *et al.* 2015).

Concluding, we find distinct and in-phase gradual perturbations of the hydro-climate system across the North Atlantic leading the transitions into the Younger Dryas stadial and the Holocene interglacial. These features imply that complex atmosphere-ocean feedbacks are at work prior to an abrupt climate change.

For Review Only

Conclusions

The Lateglacial sedimentary successions from the ancient lake at Hässeldala Port in southern Sweden spans the period 14.5-9.5 cal. ka BP and forms one of the best chronologically-constrained sites in Europe. Hässeldala Port's sediments were analysed using a variety of proxies that allow capturing local and regional climatic and environmental signals. The refined age model for the multi-proxy records (lithology, geochemistry, pollen, diatoms, chironomids, biomarkers, hydrogen isotopes) now enables discussing environmental and climatic changes in a regional context and provides a new chronological framework for the vegetation development in southern Sweden. Hässeldala Port's multi proxy records imply that regional cooling and hydroclimate changes in the Nordic Sea region led to more or less synchronous local responses in and around the ancient lake. These changes were however offset by several hundred years as compared to the start and end of Greenland stadial GS-1. Hässeldala thus provides further insights into the spatial and temporal complexity of environmental and hydroclimatic responses to North Atlantic rapid climate shifts.

References

Ammann, B., van Raden, U. J., Schwander, J., Eicher, U., Gill, A., Bernasconi, S. M., van Leeuwen, J. F. N., Lischke, H., Brooks, S. J., Heiri, O., Nováková, K., van Haardenbroek, M., von Grafenstein, U., Belmecheri, S., van der Knaap, W. O., Magny, M., Eugster, W., Colombaroli, D., Nielsen, E., Tinner, W. & Wright, H. E. 2013: Responses to rapid warming at Termination 1a at Gerzensee (Central Europe): Primary succession, albedo, soils, lake development, and ecological interactions. *Palaeogeography, Palaeoclimatology, Palaeoecology 391*, 111-131.

Ampel, L., Kylander, M. E., Steinthorsdottir, M. & Wohlfarth, B. 2014: Abrupt climate change and early lake development – the Lateglacial diatom flora at Hässeldala Port, southeastern Sweden. *Boreas 44*, 94-102.

Andersson, M. 2004: *Pollenstratigraphic response for tephra horizons during the last glacial – interglacial transition (LGIT) in southernmost Sweden*. M. Sc. thesis 4108, Stockholm University, 65 pp.

For Review Only

Andrén, T., Björck, S., Andrén, E., Conley, C., Zillén, L. & Ajar, J. 2011: The development of the Baltic Sea Basin during the last 130 ka. *In* Harff, J., Björck, S. & Hoth, P. (eds.): *The Baltic Sea Basin*, 75-97. Springer Verlag, Berlin/Heidelberg.

Anjar, J., Larsen, N. K., Håkansson, L., Möller, P., Linge, H., Fabek, D. & Xu, S. 2013: A ^{10}Be-based reconstruction of the last deglaciation in southern Sweden. *Boreas 43*, 132-148.

Bartolomé, M., Morenao, A., Sancho, C., Stoll, H. M., Cacho, I., Spötl, C., Belmonte, A., Edwards, R. L., Cheng, H. & Hellstrom, J. C. 2015: Hydrological change in Southern Europe responding to increasing North Atlantic overturning during Greenland Stadial 1. *Proceedings of the National Academy of Sciences 112*, 6568–6572.

Berglund, B. E. 1966: Late-Quaternary vegetation in eastern Blekinge, south-eastern Sweden. *Opera Botanica 12*, 5-180.

Berglund, B. E., Bergsten, H., Björck, S., Kolstrup, E., Lemdahl, G. & Norberg, K. 1994: Late Weichselian environmental change in southern Sweden and Denmark. *Journal of Quaternary Science 9*, 127-132.

Birks, H. H., Aarnes, I., Bjune, A. E., Brooks, S. J., Bakke, J., Kühl, N. & Birks, H. J. B. 2014: Lateglacial and early-Holocene climate variability reconstructed from multi-proxy records on Andoya, northern Norway. *Quaternary Science Reviews 89*, 108-122.

Birks, H. H., Battarbee, R. W. & Birks, H. J. B. 2000: The development of the aquatic ecosystem at Kråkenes Lake, western Norway, during the late glacial and early Holocene - a synthesis. *Journal of Paleolimnology 23*, 91-114.

Birks, H. H. & Birks, H. J. B. 2014: To what extent did changes in July temperature influence Lateglacial vegetation patterns in NW Europe? *Quaternary Science Reviews 106*, 262-277.

Björck, S. 1979: *Weichselian stratigraphy of Blekinge, SE Sweden, and water level changes in the Baltic Ice Lake*. Lund University. *LUNDQUA Thesis 7*, 248 pp.

Björck, S. 1981: A stratigraphic study of Late Weichselian deglaciation, shore displacement and vegetation history in south-eastern Sweden. *Fossils and Strata 14*, 1-93.

Björck, S. 1984: Bio- and chronostratigraphic significance of the Older Dryas Chronozone - on the basis of new radiocarbon dates. *Geologiska Föreningen i Stockholm Förhandlingar 106*, 81-91.

Björck, S. 1995: A review of the history of the Baltic Sea 13,0 to 8,0 ka BP: *Quaternary International 27*, 19-40.

Björck, S., Kromer, B., Johnsen, S., Bennike, O., Hammarlund, D., Lemdahl, G., Possnert, G., Rasmussen, T. L., Wohlfarth, B., Hammer, C. U. & Spurk, M. 1996: Synchronised terrestrial-atmospheric deglacial records around the North Atlantic. *Science 274*, 1155-1160.

Björck, S. & Möller, P. 1987: Late Weichselian environmental history in southeastern Sweden during the deglaciation of the Scandinavian ice sheet. *Quaternary Research 28*, 1-37.

Björck, S., Walker, M. J. C., Cwynar, L. C., Johnsen, S., Knudsen, K.-L., Lowe, J. J., Wohlfarth, B. & INTIMATE group members 1998: An event stratigraphy for the Last Termination in the North Atlantic region based on the

For Review Only

Greenland ice-core record: a proposal by the INTIMATE group. *Journal of Quaternary Science 13*, 283-292.

Blaauw, M. 2012: Out of tune: the dangers of aligning proxy archives. *Quaternary Science Reviews 36*, 38-49.

Blaauw, M. & Christen, J. A. 2011: Flexible paleoclimate age-depth models using an autoregressive gamma process. *Bayesian Analysis 6*, 457-474.

Blockley, P. E., Lane, C. S., Hardiman, M., Rasmussen, S. O., Seierstad, I. K., Steffensen, J. P., Svensson, A., Lotter, A. F., Turney, C. S. M., Bronk Ramsey, C. & INTIMATE group members 2012: Synchronisation of paleoenvironmental records over the last 60,000 years, and an extended INTIMATE event stratigraphy to 48,000 b2k. *Quaternary Science Reviews 36*, 2-10.

Blunier, T. & Brook, E. J. 2001: Timing of millennial-scale climate change in Antarctica and Greenland during the last glacial period. *Science 291*, 109-112.

Broecker, W. S. 1998: Paleocean circulation during the last deglaciation: a bipolar seesaw? *Paleoceanography 13*, 119-121.

Bronk Ramsey, C. 2010: *OxCal Program, v.4.1.7*. Radiocarbon accelerator unit, University of Oxford, UK.

Brooks, S. J. & Langdon, P. G. 2014: Summer temperature gradients in northwest Europe during the Lateglacial and early Holocene (15-8 ka BP) inferred from chironomid assemblages. *Quaternary International 341*, 80-90.

Davies, S. M., Wastegård, S. & Wohlfarth, B. 2003: Extending the limits of the Borrobol Tephra to Scandinavia and detection of new early Holocene tephra. *Quaternary Research 59*, 345-352.

Davies, S. M., Wohlfarth, B., Wastegård, S., Andersson, M., Blockley, S. & Possnert, G. 2004: Were there two Borrobol Tephras during the early Lateglacial period: implications for tephrochronology? *Quaternary Science Reviews 23*, 581-589.

Digerfeldt, G. 1971: The Post-Glacial development of the ancient lake at Torreberga, South Sweden. *Geologiska Föreningens i Stockholm Förhandlingar 93*, 601-624.

Engstrom, D. R., Fritz, S. C., Almendinger, J. E. & Juggins, S. 2000: Chemical and biological trends during lake evolution in recently deglaciated terrain. *Nature 408*, 161-166.

EPICA, Community Members 2006: One-to-one coupling of glacial climate variability in Greenland and Antarctica. *Nature 444*, 195-198.

Ising, J. 1998: Late Weichselian pollen stratigraphy, clay-varve chronology, radiocarbon chronology, and palaeomagnetic secular variations at Farslycke, Blekinge, southern Sweden. *GFF 120*, 321-332.

Iversen, J. 1954: The Late-Glacial flora of Denmark and its relation to climate and soil. *Danmarks Geologiske Undersogelse II, 80*, 87-119.

Jackson, S. T. & Overpeck, J. T. 2000: Responses of plant populations and communities to environmental changes of the Late Quaternary. *Paleobiology 26*, 194-220.

Juggins, S. 2013: Quantitative reconstructions in palaeolimnology: new paradigm or sick science? *Quaternary Science Reviews 64*, 20-23.

Karlatou-Charalampopoulou, A. 2016: *Vegetation responses to Late Glacial climate shifts as reflected in a high-resolution pollen record from Blekinge,*

For Review Only

south-eastern Sweden, compared with responses of other climate proxies. M. Sc. thesis 464, Lund University, 17 pp.

Knutti, R., Flückiger, J., Stocker, T. F. & Timmermann, A. 2004: Strong hemispheric coupling of glacial climate through freshwater discharge and ocean circulation. *Nature 430*, 851-856.

Kolstrup, E. 1979: Herbs as July temperature indicators for parts of the pleniglacial and late-glacial in The Netherlands. *Geologie en Mijnbouw 58*, 377-380.

Kolstrup, E. 1980: Climate and stratigraphy in northwestern Europe between 30.000 B.P. and 13,000 B.P., with special reference to the Netherlands. *Mededelingen Rijks Geologische Dienst 32-15*, 181-253.

Kylander, M. E., Klaminder, J., Wohlfarth, B. & Löwemark, L. 2013: Geochemical responses to paleoclimatic changes in southern Sweden since the late glacial: the Hässeldala Port lake sediment record. *Journal of Paleolimnology 50*, 57-70.

Lane, C. S., Brauer, A., Blockley, S. P. E. & Dulski, P. 2013: Volcanic ash reveals time-transgressive abrupt climate change during the Younger Dryas. *Geology 41*, 1251-1254.

Lohne, Ø. S., Mangerud, J. & Birks, H. H. 2013: Precise ^{14}C ages of the Vedde and Saksunarvatn ashes and the Younger Dryas boundaries from western Norway and their comparison with the Greenland Ice Core (GICC05) chronology. *Journal of Quaternary Science 28*, 490-500.

Lohne, Ø. S., Mangerud, J. & Birks, H. H. 2014: IntCal13 calibrated ages of the Vedde and Saksunarvatn ashes and the Younger Dryas boundaries from Kråkenes, western Norway. *Journal of Quaternary Science 29*, 506-507.

Lowe, J. J., Rasmussen, S. O., Björck, S., Hoek, W. Z., Steffensen, J. P., Walker, M. J. C., Yu, Z. & INTIMATE group members 2008: Synchronisation of palaeoenvironmental events in the North Atlantic region during the Last Termination: a revised protocol recommended by the INTIMATE group. *Quaternary Science Reviews 27*, 6-17.

Lowe, J. J., Bronk Ramsey, C., Housley, R., Lane, C. S. & Tomlinson, E. 2015: The RESET project: constructing a European tephra lattice for refined synchronisation of environmental and archaeological events during the last c. 100 ka. *Quaternary Science Reviews 118*, 1-17.

Lundqvist, J. & Wohlfarth, B. 2001: Timing and east-west correlation of south Swedish ice marginal lines during the Late Weichselian. *Quaternary Science Reviews 20*, 1127-1148.

Mangerud, J., Andersen, S. T., Berglund, B. E. & Donner, J. J. 1974: Quaternary stratigraphy of Norden, a proposal for terminology and classification. *Boreas 3*, 109-128.

Matthews, I. P., Birks, H. H., Bourne, A. J., Brooks, S. J., Lowe, J. J., MacLoed, A. & Pyne-O'Donnell, S. D. F. 2011: New age estimates and climatostratigraphic correlations for the Borrobol and Penifiler Tephras: evidence from Abernethy Forest, Scotland. *Journal of Quaternary Sciences 26*, 247-252.

Möller, P. 1987: Moraine morphology, till genesis, and deglaciation pattern in the Åsnen area, south-central Småland, Sweden. *LUNDQUA Thesis 20*, 146 pp.

Muscheler, R., Adolphi, F. & Knudsen, M.F. 2014: Assessing the differences between the IntCal and Greenland ice-core time scales for the last 14,000 years via the common cosmogenic radionuclide variations. *Quaternary*

For Review Only

Science Reviews 106, 81–87.
Muschitiello, F., Andersson, A., Wohlfarth, B. & Smittenberg, R. H. 2015a: The C_{20} highly branched isoprenoid biomarker – A new diatom-sourced proxy for summer trophic conditions? *Organic Geochemistry 81*, 27-33.
Muschitiello, F., Pausata, F. S. R., Smittenberg, R. H., Salih, A. A. M., Watson, J. E., Brooks, S. J., Whitehouse, N. J., Karlatou-Charalampopoulou, A. & Wohlfarth, B. 2015b: Fennoscandian freshwater control on Greenland hydrological shifts at the onset of the Younger Dryas. *Nature Communications* 6, 8939.
Muschitiello, F. & Wohlfarth, B. 2015: Time-transgressive environmental shifts across Northern Europe at the onset of the Younger Dryas. *Quaternary Science Reviews 109*, 49-56.
Pearce, C., Seidenkrantz, M. S., Kuijpers, A., Massé, G. & Reynisson, N. F. 2013: Ocean lead at the termination of the Younger Dryas cold spell. *Nature Communications 4*, p. 1664.
Pyne-O'Donnell, S. D. F. 2010: The taphonomy of Last Glacial–Interglacial Transition (LGIT) distal volcanic ash in small Scottish lakes. *Boreas 40*, 131-145.
Pyne-O'Donnell, S. D. F., Blockley, S. P. E., Turney, C. S. M. & Lowe, J. J. 2008: Distal volcanic ash layers in the Lateglacial Interglacial (GI-1): problems of stratigraphic discrimination. *Quaternary Science Reviews 27*, 72-84.
Rach, O., Brauer, A., Wilkes, H. & Sachse, D. 2014: Delayed hydrological response to Greenland cooling at the onset of the Younger Dryas in western Europe. *Nature Geoscience 7*, 109-112.
Rasmussen, S. O., Bigler, M., Blockley, S. P. E., Blunier, T., Buchardt, S. L., Clausen, H. B., Cvijanovic, I., Dahl-Jensen, D., Johnsen, S. J., Fischer, H., Gkinis, V., Guillevic, M., Hoek, W. Z., Lowe, J. J., Pedro, J., Popp, T., Seierstad, I. K., Steffensen, J. P., Svensson, A. M., Vallelonga, P., Vinther, B. M., Walker, M. J. C., Wheatley, J. J. & Winstrup, M. 2014: Stratigraphic framework for robust naming and correlation of abrupt climatic changes during the last glacial period based on three synchronized Greenland ice core records. *Quaternary Science Reviews 106*, 14-28.
Reimer, P. J., Bard, E., Bayliss, A., Warren Beck, J. W., Blackwell, P. G., Bronk Ramsey, C., Buck, C. E., Cheng, H., Lawrence Edwards, R. L., Friedrich, M., Grootes, P. M., Haflidason, H., Hajdas, I., Hatté, C., Heaton, T. J., Hoffmann, D. L., Hogg, A. G., Hughen, K. A., Kaiser, K. F., Kromer, B., Manning, S. W., Niu, M., Reimer, R. W., Richards, D. A., Scott, E. M., Southon, J. R., Staff, R. A., Turney, C. S. M. & van der Plicht, J. 2013: INTCAL13 and MARINE13 Radiocarbon age calibration curves 0–50,000 years cal BP. *Radiocarbon 55*, 1869–1887.
Ringberg, B. 1991: Late Weichselian clay varve chronology and glaciolacustrine environment during deglaciation in southeastern Sweden. *Sveriges Geologiska Undersökning 79*, 1-42.
Steffensen, J. P., Andersen, K. A., Bigler, M., Clausen, H. B., Dahl-Jensen, D., Fischer, H., Goto-Azuma, K., Hansson, M., Johnsen, S. J., Jouzel, J., Masson-Delmotte, V., Popp, T., Rasmussen, S. O., Röthlisberger, R., Ruth, U., Stauffer, B., Siggaard-Andersen, M. L., Sveinbjörnsdóttir, A. E., Svensson, A. and White, J. W. C. 2008: High-resolution Greenland ice core data show abrupt climate change happens in few years. *Science 321*, 680-684.

For Review Only

Steinthorsdottir, M., de Boer, A., Oliver, K. I. C., Muschitiello, F., Blaauw, M., Reimer, P. J. & Wohlfarth, B. 2014: Synchronous records of pCO_2 and $\Delta^{14}C$ suggest rapid, ocean-driven pCO_2 fluctuations at the onset of Younger Dryas. *Quaternary Science Reviews 99*, 84-96.

Steinthorsdottir, M., Wohlfarth, B., Kylander, M., Blaauw, M. and Reimer, P. J. 2013: Stomatal proxy record of CO_2 concentrations from the Last Termination suggests an important role for CO_2 at climate change transitions. *Quaternary Science Reviews 68*, 43-58.

Stocker, T. F. & Johnsen, S. J. 2003: A minimum thermodynamic model for the bipolar seesaw. *Paleoceanography 18*, 1944-9186.

Walker, M. J. C., Björck, S., Lowe, J. J., Cwynar, L. C., Johnsen, S., Knudsen, K.-L., Wohlfarth, B. & INTIMATE group members 1999: Isotopic 'events' in the GRIP ice core: a stratotype for the Late Pleistocene. *Quaternary Science Reviews 18*, 1143-1150.

Walker, M. J. C., Lowe, J. J., Blockley, S. P., Bryant, C., Coombes, P., Davies, S. M., Hardiman, M., Turney, C. S. M. & Watson, J. 2012: Lateglacial and early Holocene palaeoenvironmental 'events' in Sluggan Bog, Northern Ireland: comparisons with the Greenland NGRIP GICC05 event stratigraphy. *Quaternary Science Reviews 36*, 124-138.

Watson, J. 2008: *Quantifying Late Glacial climate change in Northwestern Europe using two insect proxies.* Ph. D. thesis, The Queen's University of Belfast, 365 pp.

Wohlfarth, B. 1996: The chronology of the Last Termination: a review of high-resolution terrestrial stratigraphies. *Quaternary Science Reviews 15*, 267-284.

Wohlfarth, B., Björck, S., Lemdahl, G. & Ising, J. 1994: Ice recession and depositional environment in the Blekinge archipelago of the Baltic Ice Lake. *GFF 116*, 3-12.

Wohlfarth, B., Blaauw, M., Davies, S. M., Andersson, M., Wastegård, S., Hormes, A. & Possnert, G. 2006: Constraining the age of Lateglacial and early Holocene pollen zones and tephra horizons in southern Sweden with Bayesian probability methods*. Journal of Quaternary Science 21*, 321-334.

Wohlfarth, B. & Possnert, G. 2000: AMS radiocarbon measurements from Swedish varved clays. *Radiocarbon 42*, 323-333.

For Review Only

Figure captions

Figure 1. A. Location of the study area in southern Sweden. B. Topography around Hässeldala Port's peatbog. C. Close-up of Hässeldala Port's peatbog showing the location of the cored successions (see Table 1 for details on the different sequences). All studied profiles were derived from the deepest part of the bog. Present-day lakes are shown in blue and peat bogs in a light brown colour. Elevations around Hässeldala Port reach between 35 and 80 m above present day sea level (a.s.l.).

Figure 2. Lithostratigraphy, total organic carbon (TOC) and loss-on-ignition (LOI) for Hässeldala Port's core #2 (Wohlfarth *et al.* 2006) and #5 (Steinthorsdottir *et al.* 2013). The brown and grey shaded rectangles mark the distinct patterns that can be recognised in all profiles. See Fig. 1C for the location of the cores.

Figure 3. A. TOC/LOI (%) curves for cores #1, #2, #3, #HP4, #5, and #6 according to depth. The brown and grey shaded rectangles mark the distinct patterns that can be recognised in all profiles. See Table 1 for references for each analysed sediment core. B. TOC/LOI (%) curves for cores #1, #2, #3, #HP4, #5, and #6 shown on the revised chronology for core #5 (Muschitiello *et al.* 2015b) (see text and Fig. 4). The grey shaded area shows those parts of the profiles, where the age was interpolated using known sedimentation rates. Tephra layers that have been geochemically identified are the Askja-S tephra (AsT), the Hässeldala tephra (HDT) and the Borrobol tephra (BT) (Davies *et al.* 2003, 2004; Wohlfarth *et al.* 2006), while other tephras in core #1 and #HP4 have not been further analysed. None of these tephras has been used in the construction of the age model.

Figure 4. Age model of Hässeldala Port's composite radiocarbon-dated succession using the IntCal13 calibration curve (Reimer *et al.* 2013). Circles indicate calibrated ^{14}C dates used to construct the age model. Blue colored circles refer to dates that were transferred from core #2 onto core #5's depth scale. The orange dotted lines show the 95% confidence bounds of the model, and the red

For Review Only

dotted line the modelled weighted mean age. See Table 3 for details on all ^{14}C dates.

Figure 5. Shoreline displacement and relative timing of the deglaciation in Blekinge province, southernmost Sweden during the regional Bølling and Older Dryas pollen zones. See Table 5 for details of all sites shown here. A. Ice recession lines (white dashed line) according to the stacked local clay-varve chronology (Ringberg 1991). The formation of the highest coastline of the Baltic Ice Lake estimated at 65-67 m a.s.l. (blue line) corresponds approximately to local varve years -10 to +10, i.e. to a position of the active ice margin around Farslycke and sites 171 and 172. The white shaded part shows the extension of the former ice sheet. B. Ice recession lines (white dashed line) according to the stacked local clay-varve chronology (Wohlfarth *et al.* 1994). The shoreline at 50-55 m a.s.l. (orange line) formed coincident with the deposition of the thick varves (local varve years +88 to +220). By this time, the active ice margin was located to the north of the study region, but stagnant ice remained above the highest coastline (Björck & Möller 1987). C. Land uplift around Hässeldala Port during the last deglaciation and location of the site in respect to the former coastlines of the Baltic Ice Lake. A. The coastline at 50-55 m a.s.l. (orange line) corresponds to the end of the regional Bølling pollen zone. D. The coastline at 45-50 m a.s.l. (dark green line) corresponds to the regional Older Dryas pollen zone. During the early part of the regional deglaciation Hässeldala Port was situated in an archipelago in the Baltic Ice Lake, but soon became part of a more continuous land area.

For Review Only

Figure 6. Hässeldala Port's lithostratigraphy and multi-proxy records shown on the revised chronology of core #5. A. Simplified lithostratigraphy of core #5. The lowermost unit 1 was only present in cores #1-3 and HP4 (see Figs 2 and 3A, B for details) and has been interpolated to core #5. B. Loss-on-ignition (LOI) curve for core #5. C. Reconstructed pH, diatom assemblage zones (DAZ-I to DAZ-IV) and crysophyte:diatom (C:D) ratios for core #5 (Ampel *et al.* 2014). D. Leaf-wax derived hydrogen isotope parameters for aquatic (δD_{n}-C_{21}) and terrestrial plants (δD_{n}-$C_{27\text{-}29\text{-}31}$) and calculated terrestrial evaporation ($\Delta\delta D_{terr\text{-}aq}$) for core #5

(Muschitiello *et al.* 2015b). All proxies in B-D were analysed on the same split samples. E. Chironomid-derived mean summer surface water temperatures for core #HP4 (Watson 2008) are shown on the revised core #5 chronology. F. Geochemically determined cryptotephra layers (AsT = Askja-S tephra; HDT = Hässeldala tephra; BT = Borrobol tephra) in cores #1-3 (Davies *et al.* 2003; 2004; Wohlfarth *et al.* 2006) are shown on the timescale of core #5 using the core-to-core alignment described in the text. G. The presence/absence of charcoal and of *Betula pubescens* and *Pinus sylvestris* macrofossils in core #2 is here shown on the timescale of core #5. H. Local pollen assemblage zones (HÄP-1 to HÄP-7) of core #3 (Andersson 2004; Wohlfarth *et al.* 2006) plotted on the revised core #5 chronology. I. Local pollen assemblage zones of core #6 (Karlatou-Charalampopoulou 2016) plotted on the revised core #5 chronology. J. Regional pollen zones (Björck & Möller 1987) and inferred Lateglacial and early Holocene vegetation in southern Sweden.

Figure 7. Age estimates for Allerød-Younger Dryas pollen zone transitions (one sigma) inferred from well-dated North European pollen stratigraphic sites (green bars): Kråkenes (Birks *et al*. 2000); Madtjärn (Björck *et al.* 1996); Sluggan Bog (Walker *et al.* 2012) and Meerfelder Maar (Rach *et al.* 2014). The age of the local pollen zone Hä-3 (brown bar) in Hässeldala Port (Karlatou-Charampopoulou 2016), which is a transitional zone between the regional Allerød and Younger Dryas pollen zones, is shown for comparison. Age estimates for the onset of Greenland Interstadial 1a (GI-1a) and Greenland Stadial 1 (GS-1) are expressed on the IntCal13 time scale after synchronization with the GICC05 scale (Muscheler *et al.* 2014).

Figure 8. Comparison of Lateglacial and early Holocene vegetation and hydroclimate changes as reconstructed from Hässeldala Port (HÄ) (Muschitiello *et al.* 2015b) and Meerfelder Maar (MFM) (Rach *et al.* 2014) compared to the Greenland event stratigraphy (displayed and plotted on the IntCal13 time scale - Muscheler *et al.* 2014). The red star marks the position of the Vedde Ash in Meerfelder Maar and in the NGRIP ice core.

For Review Only

For Review Only

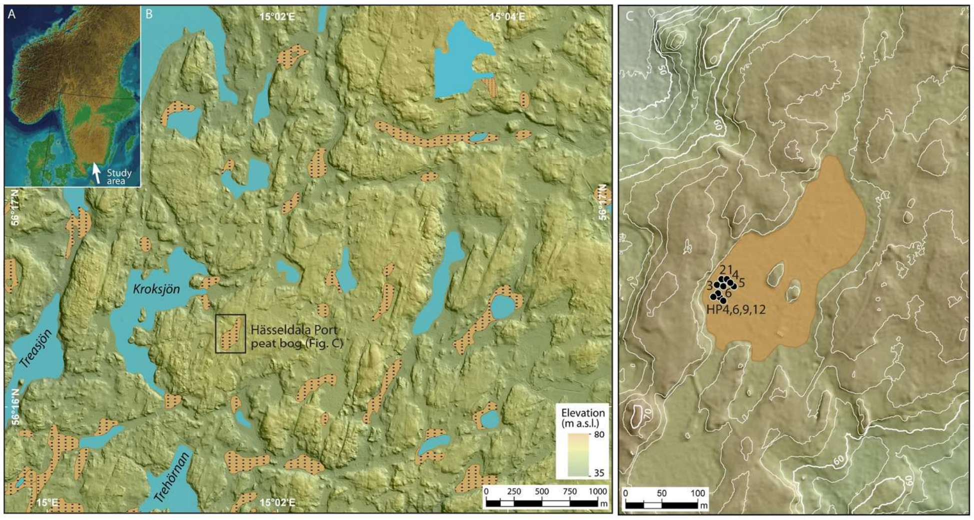

168x91mm (300 x 300 DPI)

view Only

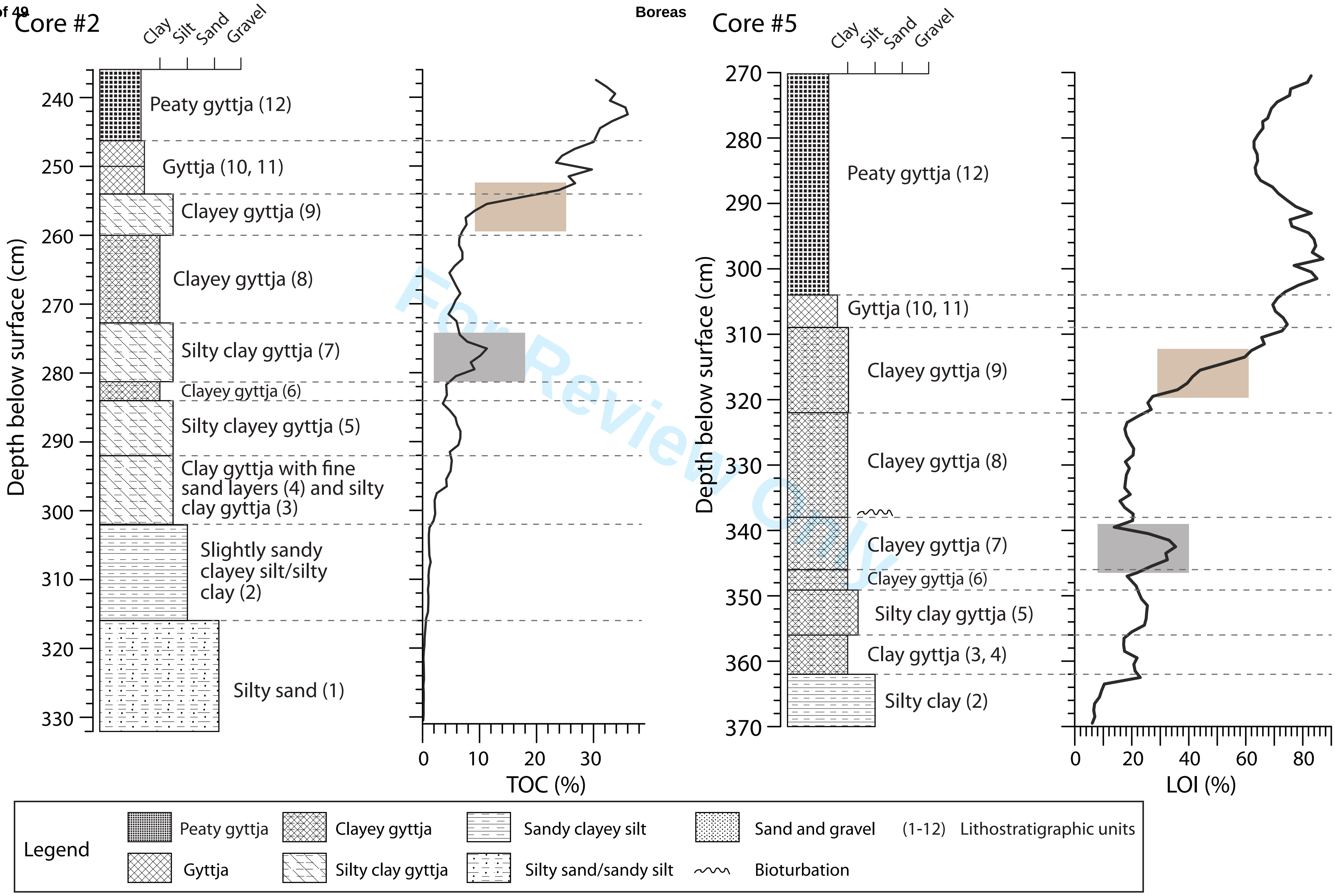

For Review Only

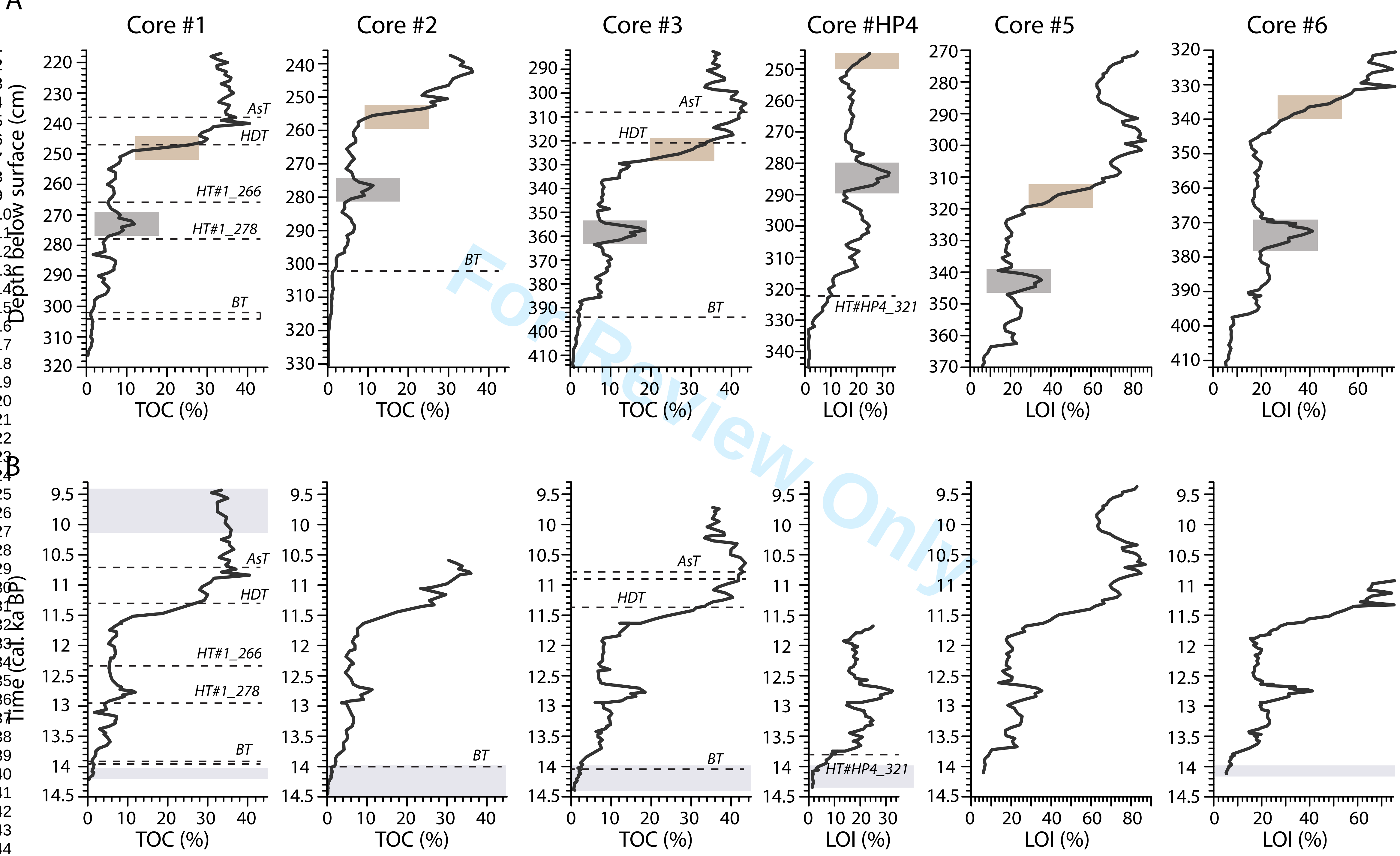

For Review Only

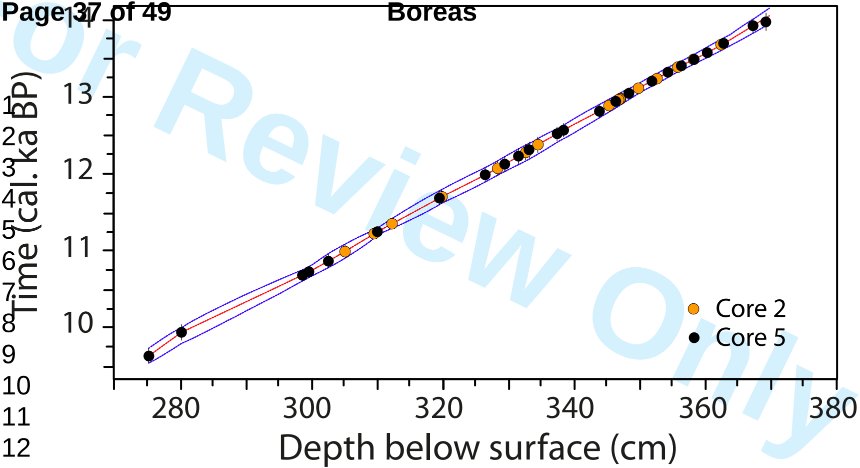

For Review Only

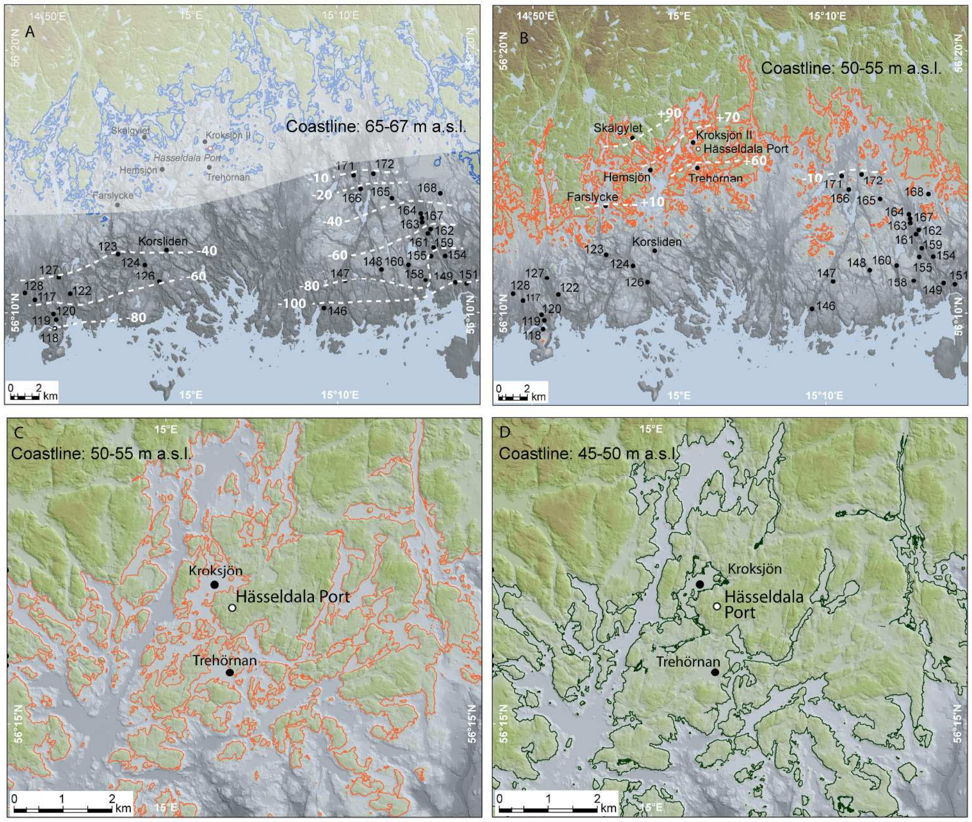

288x283mm (300 x 300 DPI)

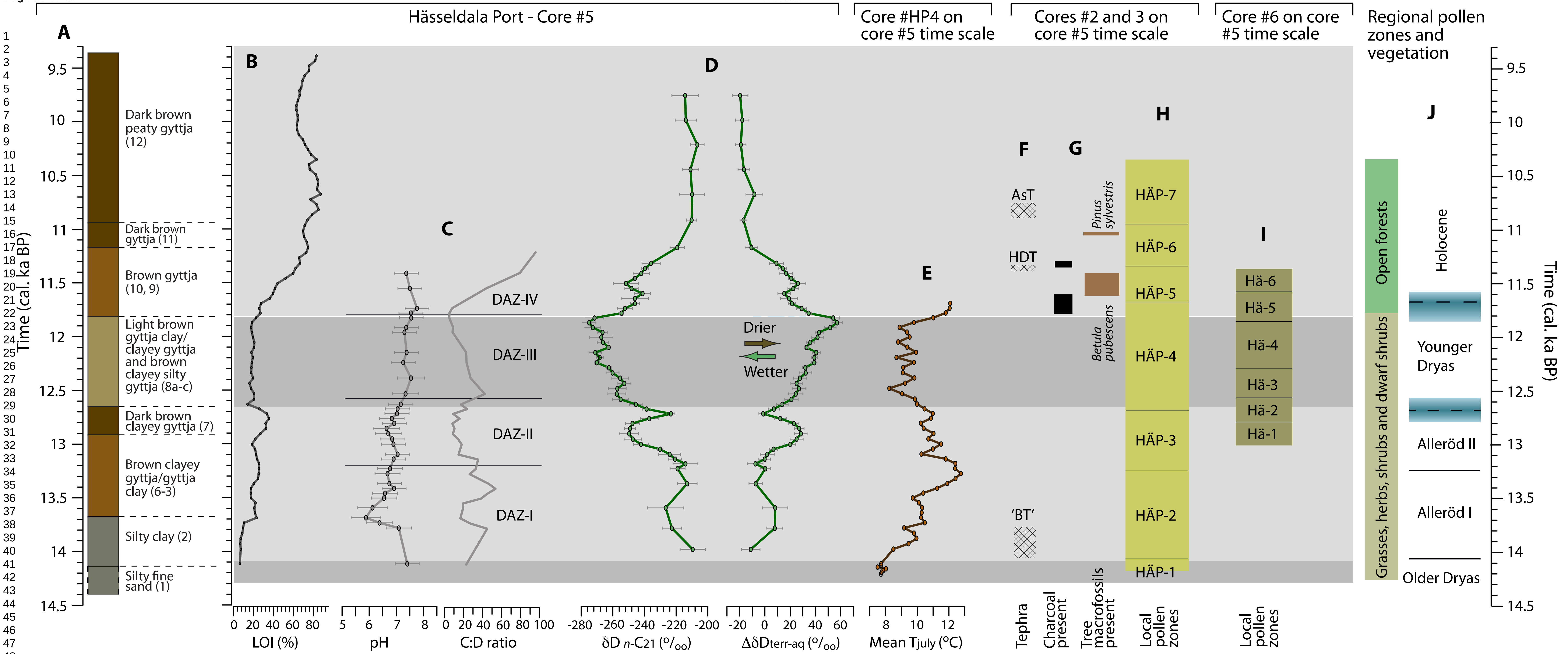
Hässeldala Port - Core #5
Core #HP4 on core #5 time scale
Cores #2 and 3 on core #5 time scale
Core #6 on core #5 time scale
Regional pollen zones and vegetation
A
B
C
D
E
F
G
H
I
J
Time (cal. ka BP)
9.5
10
10.5
11
11.5
12
12.5
13
13.5
14
14.5
Dark brown peaty gyttja (12)
Dark brown gyttja (11)
Brown gyttja (10, 9)
Light brown gyttja clay/ clayey gyttja and brown clayey silty gyttja (8a-c)
Dark brown clayey gyttja (7)
Brown clayey gyttja/gyttja clay (6-3)
Silty clay (2)
Silty fine sand (1)
DAZ-IV
DAZ-III
DAZ-II
DAZ-I
Drier
Wetter
AsT
HDT
'BT'
Pinus sylvestris
Betula pubescens
HÄP-7
HÄP-6
HÄP-5
HÄP-4
HÄP-3
HÄP-2
HÄP-1
Hä-6
Hä-5
Hä-4
Hä-3
Hä-2
Hä-1
Open forests
Grasses, herbs, shrubs and dwarf shrubs
Holocene
Younger Dryas
Alleröd II
Alleröd I
Older Dryas
LOI (%)
pH
C:D ratio
δD n-C21 (‰)
ΔδDterr-aq (‰)
Mean Tjuly (°C)
Tephra
Charcoal present
Tree macrofossils present
Local pollen zones
Local pollen zones

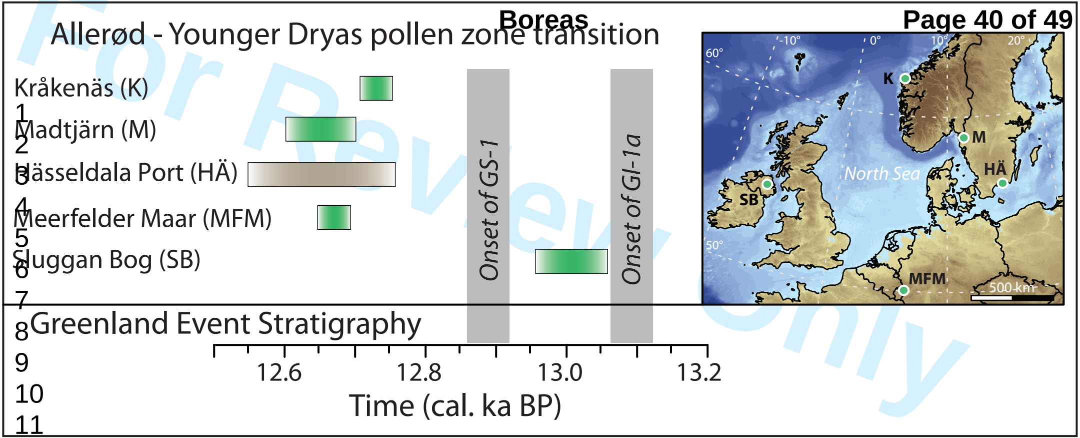

For Review Only

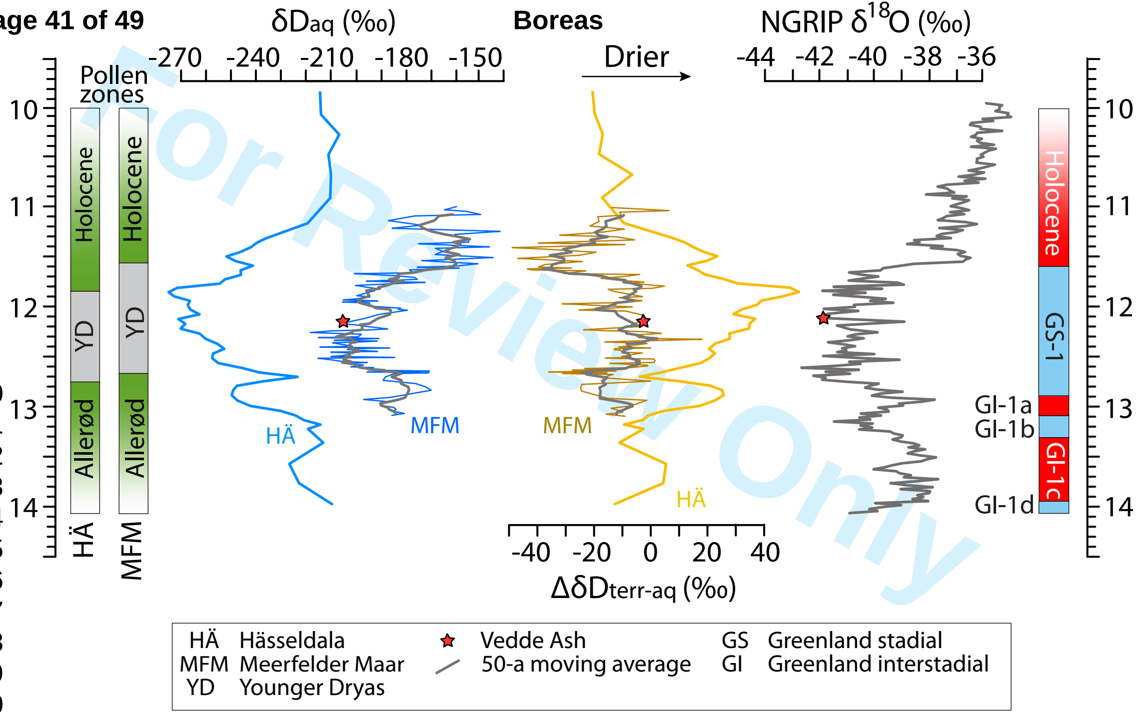

For Review Only

Table 1. Hässeldala Port sedimentary successions and analysed proxies. LOI = loss-on-ignition; TOC = total organic carbon; C/N = carbon:nitrogen ratio; XRF = major elements. Watson (2008) obtained a total of 14 parallel sediment cores from Hässeldala and sampled six of these for coleoptera analysis, two for tephra, four for LOI, and one for chironomids (#HP4). Correlation between these cores was based on stratigraphic correlations and on the pattern of the respective LOI curves (Watson 2008). See Fig. 1C for the location of the various cores.

Core #	Proxy	Reference
1	LOI, TOC, tephra	Davies *et al.* (2003)
2	TOC, tephra, ^{14}C	Davies *et al.* (2004)
3	TOC, tephra, pollen stratigraphy	Davies *et al.* (2004); Andersson (2004), Wohlfarth *et al.* (2006)
4	TOC, C/N, $\delta^{13}C_{bulk}$, $\delta^{15}N_{bulk}$, XRF	Kylander *et al.* (2013)
HP4	LOI, tephra, chironomids	Watson (2008), Muschitiello *et al.* (2015b)
HP6	LOI	Watson (2008)
HP9	LOI, tephra	Watson (2008)
HP12	LOI	Watson (2008)
5	LOI, ^{14}C, leaf stomata	Steinthorsdottir *et al.* (2013, 2014)
	Diatoms	Ampel *et al.* (2014)
	XRF	Unpublished
	Biomarkers	Muschitiello *et al.* (2015a, b)
	δD_{wax}, $\delta^{13}C$	Muschitiello *et al.* (2015b)
6	LOI, pollen stratigraphy	Muschitiello *et al.* (2015b); Karlatou-Charalampopoulou (2016)

For Review Only

Table 2. Cryptotephra found in Hässeldala Port's sediments (Davies *et al.* 2003, 2004) and Watson (2008). The Askja-S tephra (AsT), the Hässeldala tephra (HDT) and the Borrobol tephra (BT) have been geochemically identified in cores #1, 2 and 3 (Davies *et al.* 2003, 2004). Other cryptotephra layers found in cores #1 and HP4 could not be geochemically identified. See Fig. 1C for the location of the cores and Fig. 3A for details on the position of the individual tephra horizons. Tephra shard concentrations peak in core #1 at 304-303 cm depth, but remain high as far as 301 cm depth. Note that Matthews *et al.* (2011) suggested that Hässeldala Port's BT is younger than the BT found in Scotland and likely an equivalent to the Penifiler tephra.

Cryptotephra	Core #1 depth (cm)	Core #2 depth (cm)	Core #3 depth (cm)	Core #HP4 depth (cm)
Askja-S (AsT)	HT#1_238		HT#3_308-310	
Hässeldala (HDT)	HT#1_247		HT#3_ 321-322	
NN	HT#1_266			
NN	HT#_278			
NN				HT#HP4_321
Borrobol (BT)	HT#1_304-303 (302-301)	HT#2_302	HT#3_394	

For Review Only

Table 3. AMS ^{14}C dates for Hässeldala Port based on selected terrestrial plant remains and used to construct the composite age-depth model (Wohlfarth *et al.* 2006; Muschitiello *et al.* 2015b). Sample ID's shown in italics refer to dates that were transferred from core #2 to core #5 (see Fig. 4). However not all of these were used to construct the age model, since some of the ^{14}C dates were clear outliers. B = *Betula nana* – leaves, leaf fragments, seeds, buds, twigs; Bi = *Betula* indet. – twigs, leaf fragments, seeds, bark; Bp = *Betula pubescens* – seeds; C = charcoal; D = *Dryas octopetala* – leaves, leaf fragments, seeds, buds; M = moss; P = *Pinus sylvestris* – needles; T = undetermined terrestrial material. The sample depth refers to core #5 and the depth shown in brackets refers to the original depth in core #2 (Wohlfarth *et al.* 2006).

Sample depth (cm)	Thickness error (cm)	Sample ID	Material analysed	^{14}C age (a)	^{14}C error (1 sigma)	Used in the age model
369.5	0.5	UBA-20296	B, D	12 211	57	Yes
367.5	0.5	UBA-20297	D, S	11 972	62	Yes
366.6 (298.45)	1.15	*Ua-20516*	B, D, T	12 355	190	No
365.25	0.75	UBA-20298	B, D, S	11 673	56	No
363	0.5	UBA-20299	B, D	11 819	57	Yes
362.65 (296.2)	1.4	*Ua-20517*	B, D	11 920	90	Yes
360.5	0.5	UBA-20300	B, D	11 735	60	Yes
360.15 (294.35)	0.75	*Ua-20518*	B, D	11 990	110	No
358.5	0.5	UBA-20301	B, D	11 614	55	Yes
358.4 (292.85)	0.95	*Ua-20519*	B	11 805	240	Yes
356.5	0.5	UBA-20302	B, D	11 565	56	Yes
356 (291)	1.1	*Ua-20520*	B	11 525	85	Yes
354.5	0.5	UBA-20303	B	11 515	65	Yes
352.85 (289)	1.2	*Ua-20521*	T	11 490	85	Yes
352	1	UBA-20304	B	11 225	60	Yes
350 (287)	1.25	*Ua-20522*	B	11 455	125	Yes
348.5	0.5	UBA-20305	B	11 118	60	Yes
347.25 (285)	1.2	*Ua-20523*	B, T	11 245	95	Yes
347.1 (283.25)	0.9	*Ua-20524*	B, T	11 275	95	Yes
346.95 (281.5)	1.05	*Ua-20525*	B	11 200	165	Yes
346.5	0.5	UBA-20306	B	10 998	63	Yes
345.5 (279.5)	1	*Ua-20526*	B, T	10 935	80	Yes
344	1	UBA-20307	B	10 894	63	Yes
339.9 (274.75)	1.8	*Ua-20527*	B, T	11 070	135	No
338.5	0.5	UBA-20308	B	10 644	58	Yes
337.5	0.5	UBA-20309	B	10 484	50	Yes
337.4 (272.1)	0.95	*Ua-20528*	B, T	10 935	80	No

For Review Only

334.55 (270.3)	0.95	*Ua-20529*	B, T	10 515	75	Yes
333.25	1.75	UBA-20310	B	10 331	51	Yes
332.7 (268.45)	1	*Ua-16740*	B	10 165	95	Yes
331.6	1.5	UBA-20311	B	10 301	57	Yes
329.5	0.5	UBA-23306	Bi	10 331	53	Yes
328.5	0.5	UBA-20312	B	10 639	51	No
328.4 (265.5)	1.05	*Ua-16745*	B, D	10 285	95	Yes
326.5	0.5	UBA-20313	B	10 130	69	Yes
323.35 (259.1)	1.15	*Ua-16747*	B	9860	85	No
319.85 (257)	1.15	*Ua-16750*	B, C	10 205	85	Yes
319.5	0.5	UBA-21574	B	10 102	67	Yes
315.9 (255)	1.1	*Ua-16752*	B, Bp, P	9720	90	No
312.25 (253)	1.1	*Ua-16761*	B, T	9955	90	Yes
310	1	UBA-22308	Bi, M	9864	47	Yes
309.5 (251)	1.15	*Ua-16766*	P	9765	85	Yes
305.05 (246.75)	1.15	*Ua-16768*	P	9625	70	Yes
302.5	0.5	UBA-21575	B	9532	59	Yes
299.5	0.5	UBA-21577	B	9442	52	Yes
298.5	0.5	UBA-21578	B	9416	47	Yes
290	1	UBA-21576	B, C	7496	55	No
280	1	UBA-23309	Bi	9129	50	Yes
275	0.5	UBA-21579	T	8605	46	Yes

For Review Only

Table 4. Core ID, core depth and modelled and estimated ages for each core from Hässeldala Port (see Fig. 1C for the location of the cores and Fig. 3A for their TOC/LOI profiles). The statistical alignment of the TOC/LOI profiles of cores #1-HP4 and #6 to core #5 using a Monte Carlo algorithm (Muschitiello *et al.* 2015a, b) allowed transferring the chronology of core #5 to each of the profiles (Fig. 3B). The sedimentation rate in the uppermost/lowermost layers in some of the profiles had to be estimated (see main text), because these parts did not overlap with core #5: [1] = sedimentation rate 23 a cm^{-1}; [2] = sedimentation rate 22 a cm^{-1}; [3] = sedimentation rate 16 a cm^{-1}.

Core ID	Core depth (cm)	Depth (cm) interval for which the age could be modelled by correlation to core #5	Modelled median age (cal. ka BP)	Depth (cm) interval for which the age was interpolated using sedimentation rates	Estimated ages (cal. ka BP)
#1	217-316			217-225[1]	9.4-10.1
		226-305	10.2-14.0		
				306-316[2]	14.0-14.2
#2	237-331	237.5-301.5	10.6-14.0		
				302.5-330.5[3]	14.0-14.5
#3	282-415	282.5-289.5	9.7-14.0		
				290.5-415[3]	14.0-14.4
#4	336-436	—	—	—	—
#HP4	245-345	245-329	11.7-14.0		
				330-345[2]	14.0-14.3
#5	270-370	278.5-369.5	9.8-14.1		
#6	320-412	320.5-410.5	10.9-14.1	410.5-411.5	14.1

For Review Only

Table 5. Clay-varve localities investigated in Blekinge province, southernmost Sweden (Björck 1981; Ringberg 1991; Wohlfarth *et al.* 1994; Ising 1998). The local varve year corresponds to the year when the respective site had become ice free and refers to the local varve chronology for Blekinge. The numbering of the sites follows Ringberg (1991). See Fig. 5A and B for the location of the sites.

Site #	Site name	Local varve year	References
146	Vieryd 1	-103	Ringberg (1991)
149	R Fornanäs 4	-102	Ringberg (1991)
151	R Angelskog 6	-100	Ringberg (1991)
154	R Folkets Hus 9	-86	Ringberg (1991)
155	R Persborg 10	-85	Ringberg (1991)
118	Sternö	-80	Ringberg (1991)
147	Hjälmseryd 2	-80	Ringberg (1991)
158	R Långkärra 13	-79	Ringberg (1991)
160	Torneryd 15	-79	Ringberg (1991)
148	Saxemara 3	-73	Ringberg (1991)
159	R Snäckebacken 14	-73	Ringberg (1991)
119	Munkahus	-72	Ringberg (1991)
120	Drösebro	-67	Ringberg (1991)
161	R Herstorp I 16	-65	Ringberg (1991)
162	R Silverforsen 17	-63	Ringberg (1991)
126	Skyekärr	-60	Ringberg (1991)
117	Stilleryd	-59	Ringberg (1991)
163	R Herstorp II 18	-52	Ringberg (1991)
128	Horsaryd	-49	Ringberg (1991)
167	R Sörby 22	-49	Ringberg (1991)
122	Gustafsborg	-48	Ringberg (1991)
124	Trensum	-48	Ringberg (1991)
164	R Herstorp III 19	-48	Ringberg (1991)
127	Karlshamn	-41	Ringberg (1991)
123	Häggarp	-41	Ringberg (1991)
	Korsliden	-39	Wohlfarth *et al.* (1994)
165	Kjettorp I 20	-37	Ringberg (1991)
168	Kallinge Järnvägen 23	-31	Ringberg (1991)
166	Trofta	-22	Ringberg (1991)
171	Härsjölund 26	-11	Ringberg (1991)
172	Tubbarp I 27	-11	Ringberg (1991)
	Farslycke	+10	Ising (1998)
	Trehörnan	+65	Wohlfarth *et al.* (1994)
	Hemsjön	+72	Wohlfarth *et al.* (1994)
	Kroksjön II	+77	Björck (1981), Wohlfarth *et al.* (1994)
	Skälgylet	+89	Wohlfarth *et al.* (1994)

For Review Only

Table 6. Plant species present in Blekinge, southernmost Sweden during the last glacial/interglacial transition according to pollen stratigraphic and plant macrofossil analyses (Björck 1981; Berglund 1966; Wohlfarth *et al.* 1994, 2006; Steinthorsdottir *et al.* 2013). Asterisk indicates finds of plant macrofossil remains.

Time interval	Plant species
>14.1 ka BP	*Artemisia, *Betula nana, *Betula pubescens, Calluna vulgaris, Caltha palustris, *Dryas octopetala, Empetrum nigrum, Ephedra, Helianthemum, Hippophaë rhamnoides, Juniperus, Plantago, Polygonum, Populus tremula, Rumex, *Salix polaris, *S. reticulata, *S. herbacea, Saxifraga, Urtica*
14.1 – 12.7 ka BP	*Artemisia, Astralagus alpinus, *Betula nana, *Betula pubescens, Calluna vulgaris, Cerstium alpinum, *Dryas octopetala, Dryopteris, *Empetrum nigrum, Ephedra, Helianthemum, Hippophaë, Isoëtes, Jasione montana, *Juniperus communis, Lycopodium, Lastrea, Myriophyllum alterniflorum, Plantago, Polygonum, Populus tremula, Potentilla palustris, Prunus padus, Pimpinella, Polypodium, Ranunculus, Rubus, *Salix polaris, *S. reticulata, *S. herbacea, Sanguisorba, Sorbus, Saxifraga, Typha latifolia, Urtica, Valeriana officinalis*
12.7 – 11.7 ka BP	*Artemisia, Astralagus alpinus, *Betula nana, Calluna vulgaris, Cerstium alpinum, Chamaenerion alpinum, *Dryas octopetala, Dryopteris, Empetrum nigrum, Ephedra, Helianthemum, Hippophaë, Jasione montana, *Juniperus communis, Lycopus europaeus, Lycopodium, Lastrea, Minuartia, Myriophyllum alterniflorum, M. spicatum, M. verticillatum, Oxytropis capestris, Oxyria digyna, *Pinus sylvestris, Plantago, Polygonum, Potentilla palustris, Populus tremula, Ranunculus, Rumex acetosella, Rubus, *Salix polaris, *S. reticulata, *S. herbacea, Sanguisorba, Sorbus, Saxifraga, Selaginella selaginoides, Urtica*
11.7 – 10 ka BP	*Artemisia, Astralagus alpinus, *Betula nana, Botumus umbellatus, Calluna vulgaris, Cerastium alpinum, Chamaenerion augustifolium, Caltha palustris, *Dryas octopetala, Dryopteris, Empetrum nigrum, Ephedra, Helianthemum, *Hippophaë, Isoëtes lacustris, *Juniperus communis, Littorella uniflora, Lycopodium, Lastrea, Menyanthes trifoliata, Myriophyllum alterniflorum, M. spicatum, M. verticillatum, *Pinus sylvestris, Polygonum, Populus tremula, Ranunculus, Rumex acetosella, Rubus fruticosus, Sanguisorba, Sorbus, *Salix polaris, *S. reticulata, Saxifraga, Typha latifolia, Urtica*

For Review Only

Table 7. Revised time scale for southern Sweden's regional Lateglacial pollen zones (Björck & Möller 1987) based on Hässeldala Port's pollen stratigraphies (Andersson 2004; Karlatou-Charampopoulou 2016) and chronology.

Regional pollen zone	Age assignment (cal. ka BP)
Younger Dryas/Preboreal transition zone	11.85-11.58
Younger Dryas	12.54-11.85
Alleröd/Younger Dryas transition zone	12.77-12.54
Alleröd II	13.24-12.77
Alleröd I	14.06-13.24
Older Dryas	>14.06

For Review Only